Investigating the role of the Smoky River watershed on past ice-jam flood regimes at the Peace-Athabasca Delta via analysis of oxbow lake sediment cores

by

Mia Simone Stratton

A thesis
presented to the University of Waterloo
in fulfillment of the
thesis requirement for the degree of
Master of Science
in
Biology (Water)

Waterloo, Ontario, Canada, 2022

Author's Declaration

I hereby declare that I am the sole author of this thesis. This is a true copy of the thesis, including any required final revisions, as accepted by my examiners.

I understand that my thesis may be made electronically available to the public.

Abstract

The Peace-Athabasca Delta (PAD) in northern Alberta has been a focus of concern for decades due to decline in frequency and magnitude of ice-jam floods that sustain ecologically and culturally significant shallow perched lakes. Recent changes to the ice-jam flood regime of the PAD have been attributed to two main stressors, river regulation and climate change, however, the relative influence of each remains a topic of much scientific debate. Hydroelectric regulation of Peace River flow by the W.A.C. Bennett Dam began in 1968 and is widely considered to be the main cause for reduced flooding at the PAD. Longer temporal perspectives provided by paleolimnological records, however, indicate a decline in flood frequency since the early 1900s as a result of climate change. A large proportion of Peace River flow at the time when spring ice-jams floods typically occur is attributed to snowmelt runoff from unregulated 'trigger tributaries' including the Smoky and Wabasca rivers. However, our current understanding of the influence of spring discharge from these tributaries on ice-jam flooding and the subsequent recharge of perched basins at the PAD is restricted to the limited hydrometric data available since 1955. To gain a broader temporal perspective of the contribution of the Smoky River to ice-jam flooding at the PAD, sediment cores from two oxbow lakes adjacent to the Little Smoky River were investigated using paleolimnological techniques. Results from loss-on-ignition, x-ray fluorescence, and grain size collectively provide sensitive indicators of shifting flood regimes in the Smoky River watershed during the past ~160-340 years. Temporal variations in flood influence at the Smoky oxbow lakes and paleolimnological records from oxbow lakes in the Wabasca River watershed and at the PAD were characterized by four distinct phases during the past ~340 years. Phases 1 (~1680-1790) and 3 (~1850-1930) were identified as intervals of stronger flood influence while Phases 2 (~1790-1850) and 4 (~1930-2019) were interpreted as intervals of weaker flood influence. Notably, the most recent transition to weaker flood influence began in the early to mid-1900s. Strong agreement between flood records from the unregulated Smoky and Wabasca river watersheds and the PAD asserts the dominant role of climate on ice-jam flood regimes at the PAD via spring discharge from unregulated upstream tributaries. This research provides additional evidence of climate as the major driver of hydrological change at the PAD and should be considered in the development of water resource management strategies and in UNESCO's upcoming decision on the future of Wood Buffalo National Park's World Heritage status.

Acknowledgments

First and foremost, I would like to thank my supervisors Dr. Roland Hall and Dr. Brent Wolfe for their continuous support whilst enduring a global pandemic and mentoring a full roster of undergraduate and graduate students. Roland, thank you for seeing me a as a person first and a student second. It is your ability to connect with and care for your students that makes you such a wonderful supervisor. Brent, your keen eye and fervor for writing have gone a long way in making this thesis compelling and impactful. Thank you for all your guidance through the writing stages and for keeping me focused on the goal at hand.

Thank you to Dr. Johan Wiklund for providing chronologies for each of my lakes and for sharing your immense knowledge and expertise in the field of paleolimnology with me. It was through our coffee chats and quick Q&A sessions at the office that I gained a deeper understanding of the methods and theory behind this project. I could not have written a comprehensive thesis without your help.

I am so grateful to all of those in the Hall/Wolfe Lab that have provided their input and assistance along the way. First, I'd like to thank our brilliant post-docs, Dr. Lauren MacDonald and Dr. Jennifer Adams for their support with writing and figure-making. Thanks to James Telford for his many talents in the field – your playfulness and ability to teach made the 2019 field season so memorable. To Mitch Kay, thank you for all your input on topics from statistics to writing structure, and for always being a resounding yes when a beer or social gathering is suggested. I think I speak for many when I say I couldn't imagine this lab group without you. I would also like to thank Cory Savage for her skillful assistance with statistical methods and R code – I would still be asking Google for help if it weren't for your generosity. Lastly, thank you to the co-op and undergraduate students Stuart Matthews, Amy Lacey, and Ava Henderson for all their hard work conducting laboratory analyses on the Smoky sediment cores.

To my friends Sarah McMaster, Izabela Jasiak, Laura Neary, and Katie Brown, thank you for your constant support and understanding. Sarah, my best friend and roommate since 1st year of undergrad, you somehow always know exactly what I need at any given moment. Thank you for caring for me so well all these years. Izabela, my Eastern-European sister, sharing all the ways in which we are alike made me feel like I was never alone. Thank you for leading the way for me in this graduate program and offering your advice. Laura, your strength and ambition are so inspiring, and I am glad to have gotten to know you beyond what a powerful woman in science you are. Lastly, Katie, thank you for skipping through grad school hand-in-hand with me. Your kindness and sense of adventure brought me so much joy even during the most challenging parts of this degree. I truly don't know how I would have made it through grad school without each of you.

To my mom, Rose Milos, thank you for believing in me and being my biggest admirer, always. You provided me with love and reassurance each and every time I called home stressing about end-of-term responsibilities. I am so proud to share your resilience and work ethic.

Finally, thank you to my partner Colin Burchill. You've helped me through my most challenging moments and made a point to celebrate each of my achievements, big or small. I cannot thank you enough for your unwavering love and support. I am so grateful to this lab for bringing together a smitten co-op student and an oblivious undergraduate researcher – so glad you finally caught on.

Dedication

To my grandparents Hilda and Steve Milos. You have devoted your lives to providing for your family and giving each of us more opportunities than you could have ever imagined for yourselves. Your selflessness and unconditional love have helped get me to where I am today.

Table of Contents

List of Figures

List of Tables

Chapter 1 – Introduction

1.1 Water security in freshwater ecosystems

Sustained water supply is essential for freshwater ecosystems including lakes, rivers, and deltas which provide a wealth of resources for wildlife and for many Indigenous Peoples who rely on these waterways for traditional ways of life. Yet, inland waters are facing staggering reductions in water supply and biodiversity due to human activities and climate change (Dudgeon et al., 2006; Woodward et al., 2010). In northwestern Canada, climatic changes are altering the timing and intensity of precipitation, evaporation, snowmelt, and seasonal ice-cover while human activities threaten landscapes with pollution, hydroelectric regulation of river flow, and consumptive water uses (Schindler et al., 2006; Schindler & Donahue, 2006). These changes are occurring during a time of rapid population growth and a consequential increasing demand for freshwater, which emphasizes the need for judicious water resource management by multiple stakeholders. A prime example of inland waters facing both anthropogenic and climate-related stressors, and in need of effective water resource management strategies, is the Peace-Athabasca Delta in northeastern Alberta.

1.2 Concerns of drying in the Peace-Athabasca Delta

The Peace-Athabasca Delta (PAD), located where the Peace and Athabasca rivers support a complex floodplain landscape, is recognized by Ramsar as a Wetland of International Importance (Figure 1.1). The majority of the delta is located within Wood Buffalo National Park (WBNP), a UNESCO World Heritage Site. Despite these designations and associated protections, the PAD has been a focus of concern for over half a century due to declining water levels in many of its perched basins, which provide essential habitat for numerous species of wildlife and hold traditional importance to the Athabasca Chipewyan First Nation, Mikisew Cree

First Nation, and Métis in the region (PADPG, 1973; Prowse & Lalonde, 1996; Prowse & Conly, 1998; Leconte et al., 2001). These concerns prompted a petition by the Mikisew Cree First Nation (MCFN) in 2014 to have WBNP added to the list of "World Heritage in Danger" (MCFN, 2014). UNESCO (2017) responded with a list of 17 recommendations for Canada to address to avoid the downgrade in World Heritage status. In response to the UNESCO recommendations, the Canadian federal government has developed an Action Plan aimed at protecting the hydrological and ecological integrity of WBNP and the PAD (IEC, 2018; Parks Canada, 2019). However, the primary cause of lake drawdown remains a topic of much scientific debate (Beltaos, 2018; Hall et al., 2019; Wolfe et al., 2020) yet is imperative to identify for effective water resource management of the delta.

Concerns of water-level drawdown center on the perched basins of the PAD. These consist of shallow lakes and wetlands positioned within the higher-elevation portions of the delta, many of which are closed-drainage and receive little to no input from open-water flooding. Rather, their water balances are largely controlled by precipitation, evaporation, and the infrequent input of river water during episodic ice-jam floods that form on the Peace River (Prowse & Lalonde, 1996; Prowse & Conly, 1998; Lamontagne et al., 2021). Recent changes to the ice-jam flood regime and lake drying at the PAD have been variably attributed to two main stressors, namely regulation of Peace River flow by the W.A.C. Bennett Dam and climate change (Beltaos, 2014, 2018; Wolfe et al., 2012, 2020).

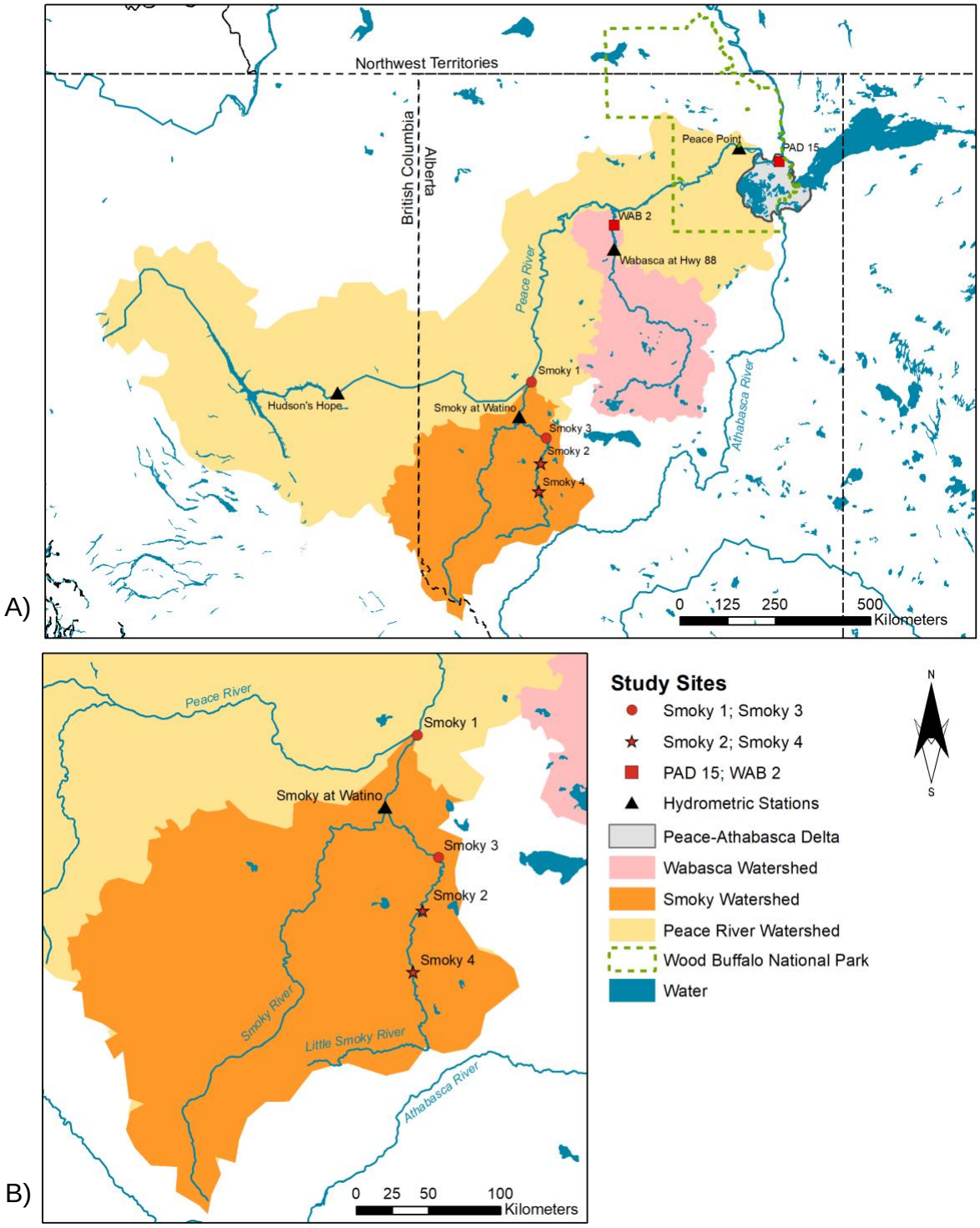

Figure 1.1 A) Map of the Peace River watershed (yellow) and two of its sub-basins, the Smoky/Wapiti (orange) and the Wabasca (pink). Also shown are the Peace-Athabasca Delta (PAD; grey) and Wood Buffalo National Park boundary (green dashed line). Study sites Smoky 2 and Smoky 4 (red stars) are oxbow lakes located adjacent to the Little Smoky River in the Smoky River watershed. Comparison sites (red squares) PAD 15 (Wolfe et al., 2006) and WAB 2 (Girard, MSc in progress) are oxbow lakes situated in the PAD and the Wabasca River watershed, respectively. The hydrometric stations from which data were used in Figure 1.5. are indicated with black triangles. B) Map of the Smoky River watershed and the locations of the four sampled oxbow lakes.

Consensus among some researchers is that hydroelectric regulation of Peace River flow is the main cause of perched lake drawdown at the PAD via reduction in the frequency and magnitude of ice-jam floods (e.g., Leconte et al., 2001; Beltaos, 2014). Regulation of the Peace River began in 1968 with the construction of the W.A.C Bennett Dam located 1180 km upstream of the PAD near Hudson's Hope, British Columbia. Hydrometric records for the lower Peace River, initiated in the late 1950s, demonstrate the dam has increased flow during winter months and reduced flow during summer months (PADPG, 1973; Prowse & Lalonde, 1996; Peters & Prowse, 2001; Beltaos et al., 2006) (Figure 1.2). Increased discharge from the dam during winter for power generation has led to higher freeze-up levels on the Peace River, which supports the contention that ice-jam flood events are less likely to occur since dam construction because more discharge is required to generate a mechanical break-up (Beltaos et al., 2006; Beltaos & Peters, 2021). However, hydrometric data only extend 8 years prior to regulation and were retrieved from gauging stations more than 85 km upstream of the PAD. These short, sparse data limit an ability to assess the natural range of variability of pre-regulation conditions and do not directly measure or characterize the hydrological and ecological changes experienced by perched basins within the PAD.

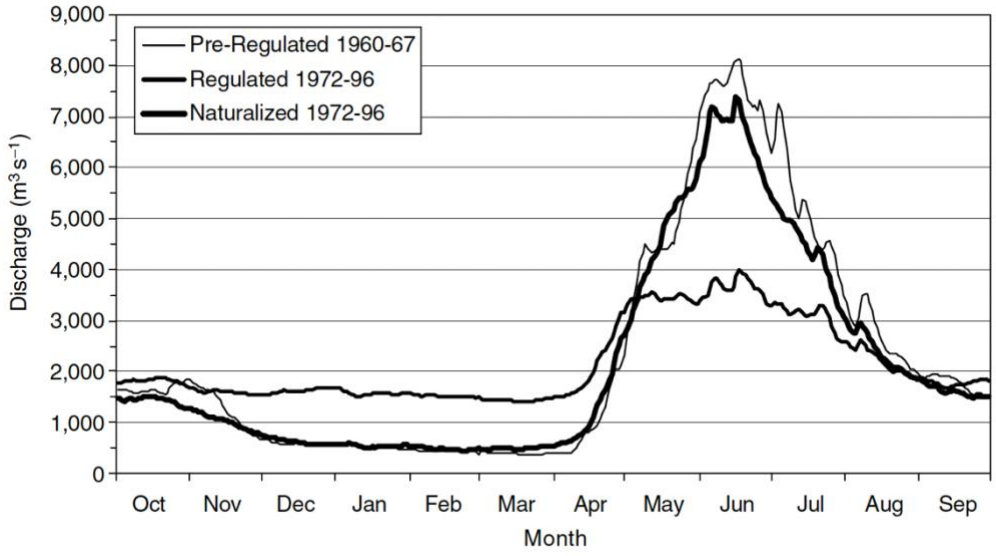

Figure 1.2. Average daily discharge for the Peace River at Peace Point during the pre-regulated (1960-1967) and regulated (1972-1996) periods as well as a modelled naturalized flow regime (1972–1996) estimating effects without regulation. The regulated period is characterized by increased discharge during winter months (November through mid-April) and reduced discharge during spring and summer months (mid-April through July). Figure 6 from Peters & Prowse (2001; pg. 3190).

Climate is the other major factor that studies have associated with reduced flooding at the PAD and drying of the perched basins. Since the late 1990s, researchers have recognized the consequences of a warming climate and have acknowledged that reductions in ice thickness, ice strength, ice-cover duration and runoff from the winter snowpack are likely contributing to milder spring break-up events which are incapable of recharging perched basins (e.g., Prowse & Lalonde, 1996; Prowse & Conly, 1998). However, disentangling the relative roles of river regulation and climate change on ice-jam flooding and, in turn, determining the most effective water management strategies, remains challenging.

To gain a longer perspective and enhance understanding of the role of climate versus river regulation, paleolimnological studies have been conducted at multiple perched basins and oxbow lakes in the PAD (reviewed in Wolfe et al., 2012; Kay et al., 2019). Oxbow lakes are the result of former meanders in a river that have since been separated through processes of erosion and deposition. Many remain flood-prone due to their proximity to the main river channel.

Studies by Kay et al. (2019) and those reviewed in Wolfe et al. (2012) examined the physical, chemical, and biological components of lake sediment to characterize past hydrologic change and have extended the historical flood record of the PAD using data collected from the individual lakes experiencing drying and those prone to flooding. Results indicated that during the past ~400 years, perched basins at the PAD experienced marked changes in hydrology, not dissimilar from the changes observed in the post-regulation period, suggesting that the recent drying trends are not outside the range of natural variation (Wolfe et al., 2005, 2006; Sinnatamby et al., 2010). A study that reconstructed flood histories of two oxbow lakes (PAD 15 & PAD 54) at the PAD found a directional shift to reduced flooding that began in the early twentieth century, several decades before construction of the W.A.C. Bennett Dam (Wolfe et al., 2006). This finding challenges the interpretations of other studies that suggest reduced ice-jam flood frequency is coincident with the timing of the dam, and as such, has been the focus of much recent debate (Beltaos, 2018; Hall et al., 2019; Wolfe et al., 2020).

1.3 Ice-jam flooding and the Smoky River

For ice-jam floods on the Peace River to inundate elevated portions of the PAD, a specific combination of hydrological conditions must occur. These factors include cold temperatures during winter to foster strong, thick river ice and a large snowpack volume within upstream portions of the watershed and subsequent rapid snowmelt to cause a substantial increase in river flow that will exceed the downstream resistance forces keeping ice-cover intact (Prowse & Conly, 1998; Lamontagne et al., 2021). It is now well understood that the majority (75-90%) of Peace River flow at the time of breakup is attributed to snowmelt runoff from unregulated tributaries including the Smoky and Wabasca rivers (PAD TS, 1996; Prowse & Conly, 1998; Lamontagne et al., 2021) (Figure 1.3). This is due to mid-elevation areas including

the Smoky/Wapiti River sub-basin (or Smoky River watershed) that experience earlier snowmelt than the regulated high elevation headwater region of the Peace River at Hudson's Hope and, thus, produce greater discharge in the spring months of April and May (Lamontagne et al., 2021). The large contribution of spring flow from the unregulated tributaries suggests they play an important role in triggering ice-jam events at the PAD.

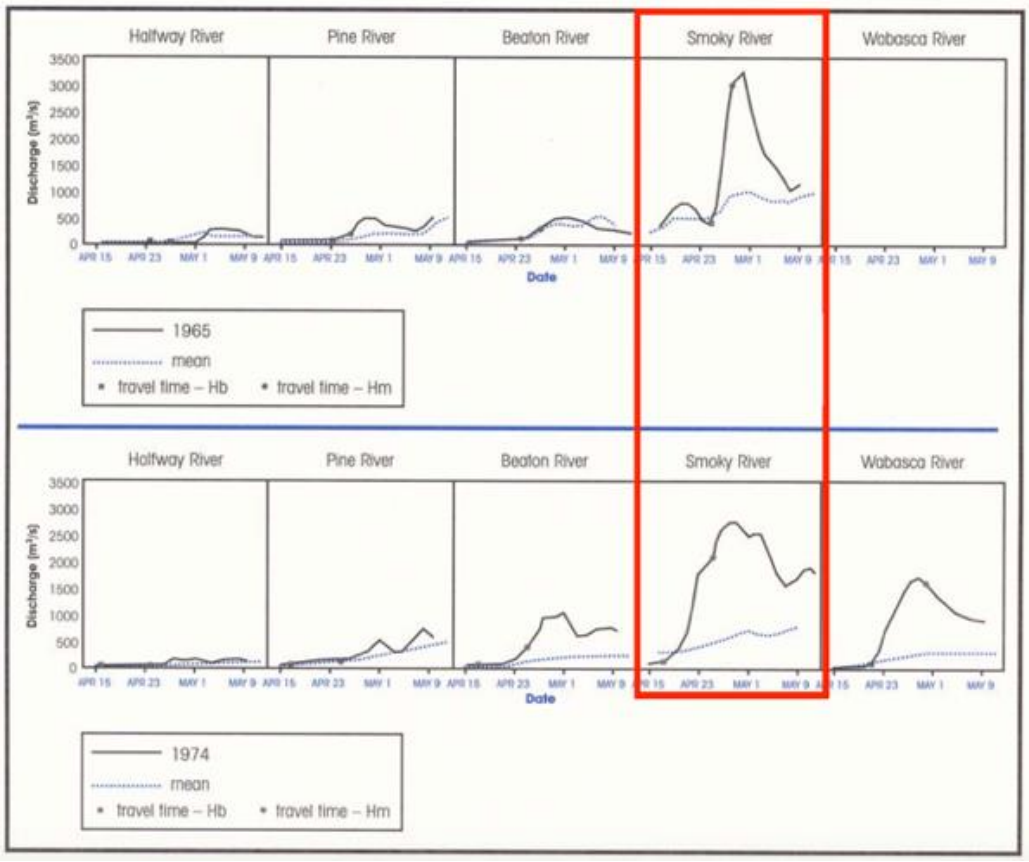

Figure 1.3. Spring hydrographs for tributaries of the Peace River in ice-jam flood years: 1965 (top) and 1974 (bottom). The Smoky River demonstrated the highest spring discharge in both years, suggesting that it may be a large contributor of discharge required for ice-jam breakup. Adapted from Figure 3.1.9 in PAD Technical Studies (1996; pg. 31).

Prior to regulation of the Peace River, the Smoky River contributed considerably more spring flow during known ice-jam flood years than did the high-elevation headwaters of the Peace River near Hudson's Hope (Prowse & Conly, 1998). During the post-regulation period, however, researchers detected marked decline of snowpack volume and melt intensity in the Smoky/Wapiti River sub-basin beginning in the mid-1970s, which was attributed to shifts in

atmospheric patterns in the North Pacific beginning in 1976 (Figure 1.4) (Prowse & Lalonde, 1996; Keller, 1997; Prowse & Conly, 1998). These findings support the claim that climate plays a key role in ice-jam formation via reduction of snowpack volume and spring discharge from the mid-elevation sub-basins, including the Smoky River watershed, and may also have contributed to the low frequency of major ice-jam flooding in the PAD during the post-1976 interval illustrated in Figure 1.4.

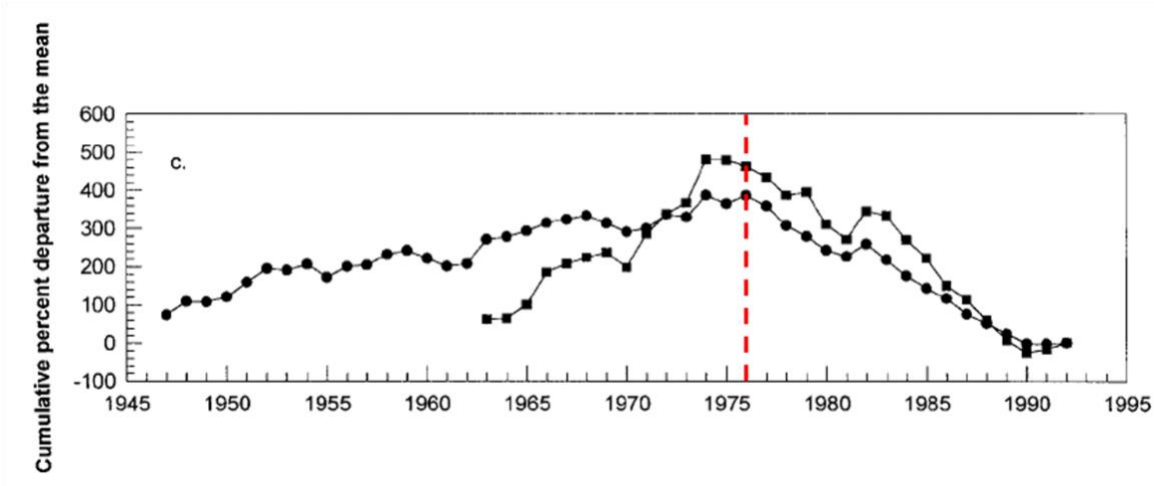

Figure 1.4. Cumulative percent departure from the mean annual maximum snowpack (squares) and winter precipitation (circles) at Grande Prairie, Alberta. Red line at 1976 indicates the beginning of atmospheric shifts in the North Pacific. Adapted from Figure 7C by Prowse & Conly (1998; pg. 1604).

To further illustrate the role of unregulated tributaries in providing spring discharge that triggers ice-jam floods at the PAD, historical flow data from multiple stations along the Peace River are shown alongside a reconstructed flood history from paleolimnological analysis of oxbow lake PAD 15 (Figure 1.5). Multiple gauging stations along the Peace River were used to extract the annual maximum daily spring discharge during the 3-week period when ice-jam floods typically occur at the PAD (Beltaos & Peters, 2020). In the lower two panels of Figure 1.5, a flood record of oxbow lake PAD 15 is illustrated using two sensitive paleolimnological methods: carbon to nitrogen (C/N) weight ratios to depict flood events since 1940 and magnetic susceptibility values dating back to ~1700 to demonstrate the benefit of an extended flood record

showing long-term trends (Wolfe et al., 2006). The hydrometric records from the Smoky and Wabasca rivers show peaks in maximum daily spring discharge that correspond to flood events recorded in the sediments at oxbow lake PAD 15, further suggesting that these tributary watersheds play a key role in triggering ice-jam floods on the Peace River at the PAD. However, our current understanding of the influence of spring discharge from unregulated tributaries on ice-jam flooding and the subsequent recharge of perched basins at the PAD is restricted to the limited hydrometric data available only since 1955. Less than 70 years of data is insufficient to assess century-long climate-driven trends such as those captured in the PAD 15 and PAD 54 sediment cores reported in Wolfe et al. (2006). To gain a deeper understanding of the Smoky River's role in ice-jam flooding at the PAD and shifting flood regimes, a longer temporal perspective of spring discharge from the Smoky River watershed is required. This would allow for the depiction of long-term climatic trends and to assess if there is evidence of declining spring discharge from the Smoky River that corresponds with decreasing flood frequency at the PAD since the early 20th century, that would otherwise be undetectable with the current limited hydrometric dataset. Such information will be pivotal in establishing appropriate water resource management strategies for the PAD and should be considered in UNESCO's upcoming decision on the future of Wood Buffalo National Park's World Heritage status.

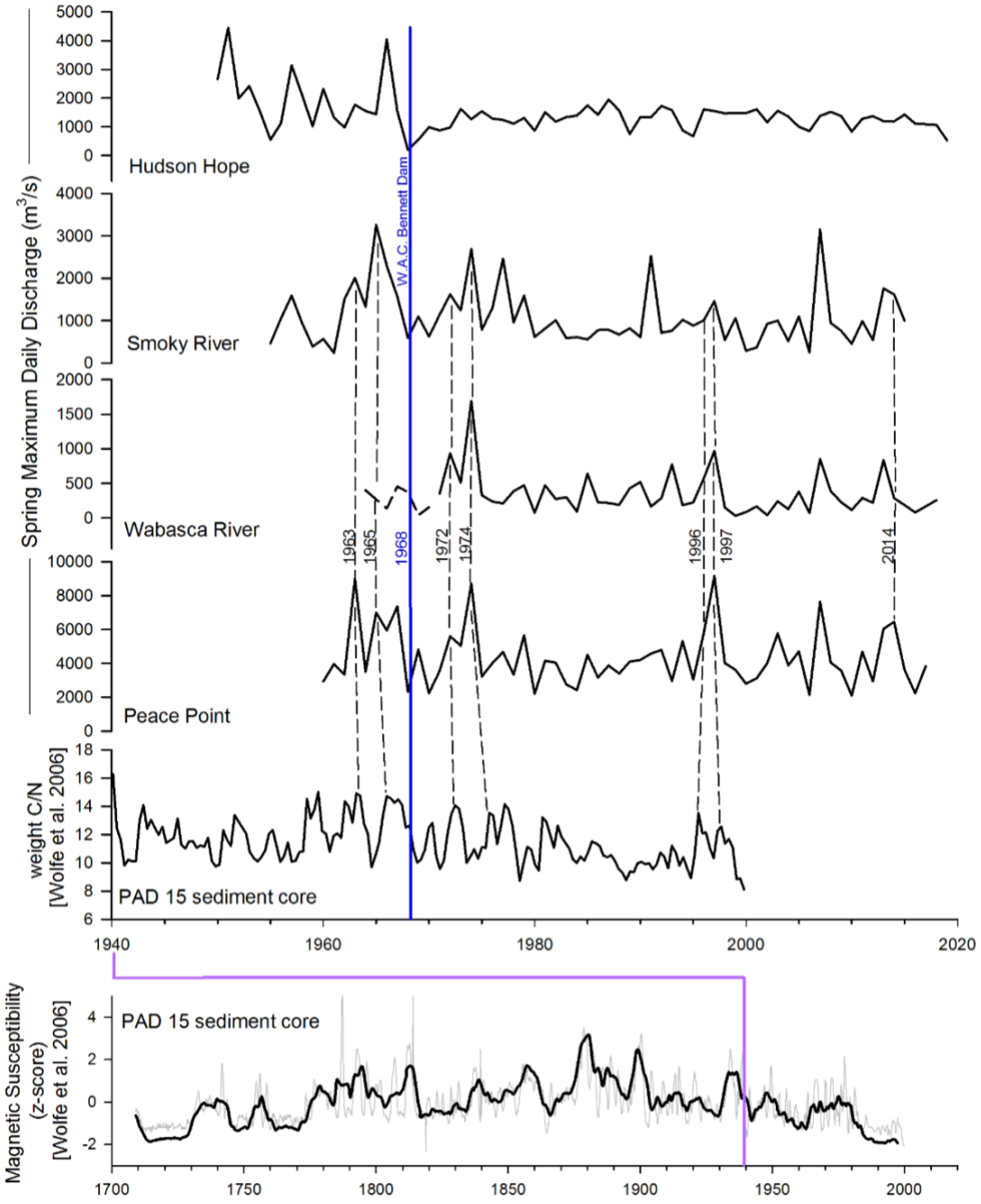

Figure 1.5. Annual maximum daily spring discharge (April 23 – May 14) at multiple stations along the Peace River (top four panels). Included are Peace River at Hudson's Hope (ID:07EF001) representing headwater flows, Smoky River at Watino (ID:07GJ001) representing flow from the Smoky River watershed, Wabasca River at Hwy No. 88 (ID: 07JD002) and Wabasca River above Peace River (ID: 07JD001) representing flow from the Wabasca River watershed, and Peace River at Peace Point (ID:07KC001) representing total flow received by the Peace River 85 km upstream of the PAD. Known ice-jam flood years are indicated next to vertical dashed lines (Timoney, 2009). Sediment core carbon/nitrogen and magnetic susceptibility records from oxbow lake PAD 15 (bottom two panels) are included to demonstrate flood events recorded within the PAD and to illustrate the benefit of an extended record showing long term trends. High C/N values indicate an influx of terrestrial organic debris introduced by floodwaters and are representative of flood events. Peaks in magnetic susceptibility z-scores are interpreted as an introduction of minerogenic, magnetic-rich detrital sediment from high-energy flood events. Hydrometric data were retrieved from https://wateroffice.ec.gc.ca/. Paleolimnological data were retrieved from Wolfe et al. (2006).

1.4 Study objectives

The objectives of this study are to: 1) reconstruct past variation in flood influence at oxbow lakes along the Little Smoky River (a tributary of the Smoky River) and 2) assess if temporal changes in flood influence from the Smoky River watershed coincide with the decline in flooding at the PAD since the early 20th century, inferred from the sediment record of oxbow lake PAD 15 (Wolfe et al., 2006). To accomplish the first objective, sediment cores from oxbow lakes in the Smoky River watershed were assessed using paleolimnological techniques to identify temporal variation in flood influence. To support the second objective, results from a concurrent study investigating the role of the Wabasca River (WAB 2; Girard, MSc in progress) will be discussed to provide a more holistic understanding of the role of unregulated upstream tributaries on ice-jam flooding at the PAD. If the timing of hydrologic changes in the Smoky River watershed coincide with those previously identified in the PAD, this will provide additional evidence that ice-jam flooding in the PAD is largely dependent on spring flow generated from upstream tributaries including the Smoky River, and that climate is the dominant driver of change in each of these systems.

Chapter 2 – Methods

2.1 Study location

The Smoky River is a major tributary of the Peace River within the Peace River watershed (Figure 1.1). The headwaters of the Smoky River are located in the Rocky Mountains at an elevation of 3,269 m and flow northeast towards the Peace River lowlands which are at an elevation of 315 m (Rokaya et al., 2020). Its confluence with the Peace River is located approximately 655 km upstream of the Peace-Athabasca Delta. Unlike the Peace River, the 492 km-long Smoky River is unregulated (Pomeroy et al., 2013). Fed largely by the Wapiti and Little Smoky rivers, the Smoky River Basin has a total area of 51,839 km^2 and drains roughly 17% of the Peace River Basin (Rokaya et al., 2020). Smoky River discharge is highest in the spring when snowmelt runoff occurs and rainfall runoff is high. Spring flows from the Smoky River are substantial compared to other contributors to Peace River flow at the time of ice-jam flood events at the PAD (Prowse & Conly, 1998; Figure 1.3). High flows are also observed in June and July when snowmelt occurs at higher elevations at the headwaters of the Smoky River (Rokaya et al., 2020).

Four candidate flood-prone oxbow lakes along the Little Smoky River in the Smoky River watershed were initially sampled for this study (Figure 2.1). The lakes were simply named Smoky 1 through Smoky 4. Due to a scarcity of flood-prone lakes in close proximity to the main Smoky River channel, study lakes were chosen adjacent to the Little Smoky River where oxbow lakes are prevalent. Smoky 1-4 were chosen based on their low sill elevation relative to the Little Smoky River, which makes them likely prone to flooding. Sediment cores retrieved from these lakes are intended to provide a record of past flood events during years of rapid snowmelt runoff and high spring discharge.

Figure 2.1. Photos of lakes sampled in the Smoky River watershed. Lakes with asterisks (Smoky 2 and Smoky 4) were chosen to be the primary focus of this study. Smoky 1 is adjacent to the confluence of the Smoky and Peace rivers. All other lakes are situated along the Little Smoky River. Approximate coring locations are indicated by a yellow diamond.

2.2 Field methods – Sediment core collection

On September 10 and 11, 2019, three sediment cores were collected from each of the four oxbow lakes. Prior to core collection, limnological measurements were taken with a YSI device (Table 2.1). Three cores were retrieved from each lake using a hammer-driven gravity corer operated from the pontoon of a helicopter (Telford et al., 2021). The lengths of the cores ranged from 36.5-79 cm (Table 2.1). A 'working core', renamed 'Core 1' (C1), was selected based on length, visible laminations, and least amount of disturbance at the surface of the core. The next-best core based on these same parameters was designated as a secondary working core (Core 2; C2) to be used if there was insufficient sediment mass from C1 to conduct all the laboratory analyses. The third core (Core 3; C3) was preserved as an archival core. Within 24 hours of

collection, all cores were sectioned into 0.5-cm intervals, which were individually sealed in Whirl-Pak® bags and refrigerated before being transported for storage in a 4°C cold room at the University of Waterloo.

Table 2.1. Lake characteristics including location, depth, core length, and limnological variables. All measurements were taken on September 10 or 11, 2019. The lakes chosen to address the research objectives of this thesis are highlighted in grey.

Lake Name	Lake Location	Lake Depth at Coring Location (m)	Length of Cores (cm)	Limnological variables at 0.4 m depth				
				Temperature (°C)	Dissolved Oxygen (%)	Specific Conductivity (µS/cm)	pH	Turbidity (FNU)
Smoky 1	56°10'18.30"N 117°20'26.70"W	1.2	C1: 61.0 C2: 54.0 C3: 42.0	14.9	85.4	328.5	8.00	37.63
Smoky 2	55° 5'37.00"N 117° 6'52.00"W	1.9	C1: 49.5 C2: 40.0 C3: 36.5	14.7	46.3	188.7	6.99	3.74
Smoky 3	55°25'6.50"N 116°59'35.90"W	1.2	C1: 57.5 C2: 51.0 C3: 51.0	14.4	43.8	646.0	7.13	3.33
Smoky 4	54°42'38.00"N 117° 9'10.60"W	1.1	C1: 64.5 C2: 57.5 C3: 60.0	14.0	53.4	328.4	7.14	1.88

Of the four oxbow lakes, two were chosen to address the research objectives of my MSc thesis based on in situ limnological measurements and loss-on-ignition results that indicated their high susceptibility to flooding. The lakes chosen to be studied further are Smoky 2 and Smoky 4, both oxbow lakes located along the Little Smoky River (Figure 1.1; Figure 2.1). For the remainder of this thesis, only the results from these two lakes will be discussed.

2.3 Sediment core analyses

2.3.1 Radioisotope dating

The working cores (C1) of Smoky 2 and Smoky 4 were radiometrically dated using ^{210}Pb, a natural radioactive isotope of lead with a half-life of 22.3 years, and ^{137}Cs and ^{241}Am, artificial radionuclides formed during above-ground nuclear bomb testing. Activity levels of ^{226}Ra, the parent isotope of ^{210}Pb, is used to estimate the supported ^{210}Pb activity. Background ^{210}Pb activity is identified at the point in which ^{226}Ra and total ^{210}Pb activity levels are equivalent.

(Appleby, 2001). Approximately 4 g of freeze-dried sediment was sub-sampled from select 0.5-cm intervals and packed into pre-weighed DSPEC tubes to a height of 35 mm. The tubes were then sealed with a silicone septum and 1 mL of epoxy and stored for at least 22 days to allow for equilibration between parent and daughter radioisotopes. Samples were then analyzed at the University of Waterloo on an Ortec HPGe Digital Gamma Ray Spectrometer using Maestro 32 software.

Ages of depth horizons were determined using the Constant Rate of Supply (CRS) model based on ^{210}Pb activity, and accuracy was improved by constraining the excess ^{210}Pb inventory using the Reference Date Method (Appleby, 2001). An independent reference date of 1963, associated with maximum atmospheric fallout from nuclear weapons testing and assumed to be identified by a peak in ^{137}Cs activity, was used to first determine the excess ^{210}Pb inventory between 1963 and 2019 (i.e., the date of core collection). The remaining excess ^{210}Pb inventory below the 1963 depth horizon was then calculated using Equations 35-36 from Appleby (2001). After constraining the total excess ^{210}Pb inventory using this method, the CRS age model was applied. The sediment chronology was extrapolated below the lowermost horizon of excess ^{210}Pb inventory using the mean dry-mass sedimentation rate determined from the cumulative dry mass between the surface of the core and the 1963 reference date horizon.

2.3.2 Loss-on-ignition analysis

Loss-on-ignition (LOI) methods, as outlined by Heiri et al. (2001), were conducted on the working cores of Smoky 2 and Smoky 4 to determine the water, organic matter, mineral matter, and carbonate content of each contiguous 0.5-cm sediment interval. Variations in each of these measurements can indicate changes in sediment composition to infer shifts in hydrological processes over time. Specifically, carbonate-free mineral matter content is used to determine the

relative influence of flooding on lakes where high mineral matter content is interpreted as periods of strong flood influence caused by the deposition of mineral-rich river sediment into lakes (Last, 2001; Wolfe et al., 2006; Kay et al., 2019).

For this procedure, 0.5-1.0 g of well-mixed wet sediment was sub-sampled and transferred to a crucible with a known mass, and the initial mass of the sample was recorded. Crucibles containing sediment then underwent a series of heat treatments, each followed by a 2-hour cooling period in a desiccator to avoid mass discrepancies associated with temperature and humidity. In the first treatment, samples were dried in an oven at 90°C for 24 hours to remove water content. The samples were then combusted in a muffle furnace at 550°C for two hours to remove the organic matter and determine the organic matter content, which was then subtracted from 100 to determine the mineral matter content. Lastly, samples were combusted in a muffle furnace at 950°C for two hours to remove carbonates. The carbonate content of the original sample was calculated by multiplying the weight loss from the 950°C step by 1.36 (Dean, 1974). To identify the carbonate-free mineral matter content of sediment, the carbonate component was subtracted from the mineral matter content. The carbonate-free mineral matter content is used to inform about past variation in flood influence in the remainder of this study.

2.3.3 Particle size analysis

Particle (or grain) size has been used in previous paleolimnological studies to track temporal variation in high-energy hydrological events (Campbell, 1998; Schnurrenberger et al., 2003; Parris et al., 2010). According to Parris et al. (2010), flood events are characterized by relatively large sediment particles due to high energy of stream inflow which carries sediment originating from bank erosion, while fine-grained sediment is typically the result of organic

matter accumulation and re-deposition of very fine-grained mineral matter in lakes under low energy conditions.

Particle size analysis was conducted on every 0.5-cm sediment interval from the working cores of Smoky 2 and Smoky 4, with duplicate analyses of sub-samples performed every 5 cm beginning at 10.0 cm. Approximately 0.3-0.6 g of wet sediment from each interval was sub-sampled into 55 mL glass tubes with phenolic screw caps. To remove organic matter, the glass tubes containing sediment were filled with sodium hypochlorite, agitated with a stir rod and left to rest in the reagent for 24 hours. Sodium hypochlorite is less likely to disintegrate minerals than other reagents such as hydrogen peroxide, thus it is the preferred reagent for analyses of mineral properties such as grain size (Mikutta et al., 2005). Once settled, the supernatant was aspirated, and samples were rinsed with deionized water. This rinsing process was repeated approximately every 48 hours until samples achieved a pH similar to the deionized water. Samples were then aspirated for a final time and suspended in approximately 5 mL of 0.1% Calgon (sodium hexametaphosphate) dispersant. The samples were then analyzed by a Horiba Partica LA-950V2 Laser Particle Size Analyzer at Wilfrid Laurier University and data were collected using the LA-950 program for Windows. Grain size data were analyzed in SigmaPlot following the surface plot method outlined in Beierle et al. (2002) to identify intervals with coarser grain size composition interpreted to be caused by input via river floodwaters.

2.3.4 X-ray fluorescence (XRF) analysis

Energy-dispersive x-ray fluorescence spectrometry (ED-XRF) was conducted on the working cores of Smoky 2 and Smoky 4 at contiguous 0.5-cm intervals to determine the trace elemental composition of the sediment. High concentrations of elements typically found in

mineral-rich sediment (Al, Si, Ti, Rb, Zr, K and Th) are used to indicate periods of strong flood influence at the oxbow lakes (e.g., Elghonimy & Sonnenberg, 2021; Peti & Augustinus, 2022).

Samples were prepared following methods described in Gregory et al. (2017). This method involves the use of an Itrax Sequential Sample Reservoir (SSR) vessel, which consists of 59 sequential acrylic compartments, each 1.5 x 1 x 1 cm (depth x length x width), aligned down the center of a clear acrylic base. Wet sediment from each 0.5-cm interval was tightly packed into the SSR compartments, sequentially from top to bottom of the core. The filled SSR vessels were covered with a layer of polyethylene film and left to settle in a cold room at 4°C until transport to McMaster University. Immediately prior to scanning, the SSR compartments were topped-up with wet sediment to ensure the samples were flush with the top of the compartment walls. The prepared SSR vessels were then analyzed at McMaster University in a Cox Itrax-XRF core scanner at a resolution of 0.20 mm (Smoky 4) and 1.00 mm (Smoky 2), using a Mo-anode x-ray tube. The resolution was decreased for Smoky 2 when results for Smoky 4 proved to be excessive with ~18 measurements taken per sediment interval. When reduced to 1.00 mm resolution, approximately 4 measurements were recorded per sediment interval.

The XRF results were batch-analyzed using RediCore software created by Cox Analytical Solutions. Count data for 56 elements were provided at each scanning point. However, scanning at each of the set resolutions included measurements taken along the 4 mm wide acrylic walls between each sediment compartment. These extraneous measurements were manually removed from the raw data and verified as illegitimate using Fe measurements where raw counts were markedly lower in acrylic wall measurements than true sediment readings. Measurements were averaged for each of the 56 elements within the individual sediment intervals.

2.4 Data analysis

2.4.1 Principal Component Analysis

A Principal Component Analysis (PCA) of the XRF data was conducted to explore the associations among elements within the sediment intervals of each lake core. Of the 56 elements included in the XRF data output, 20 were chosen to be included in the PCA based on their expected association with flood occurrence or magnitude (Davies et al., 2015) and the relative strength of their characterization by the Itrax core scanner, where most elements with counts below ~100 were excluded. The 20 elements included are as follows: Al, Ba, Br, Ca, Cr, Cu, Fe, K, Mn, Ni, Rb, Sb, Si, Sr, Th, Ti, V, W, Zn, and Zr. The PCA was conducted in 'R Studio', version 1.2.5, with the packages 'factoextra' (Kassambara & Mundt, 2020) and 'ggplot2' (Wickham, 2016). PCA axis 1 sample scores were extracted from R using the 'clipr' package (Lincoln, 2022) and plotted against the determined sediment interval dates to assess temporal patterns of variation in the elements associated with strong flood influence in the sediment cores.

Chapter 3 – Results & Interpretation

3.1 Sediment core chronologies

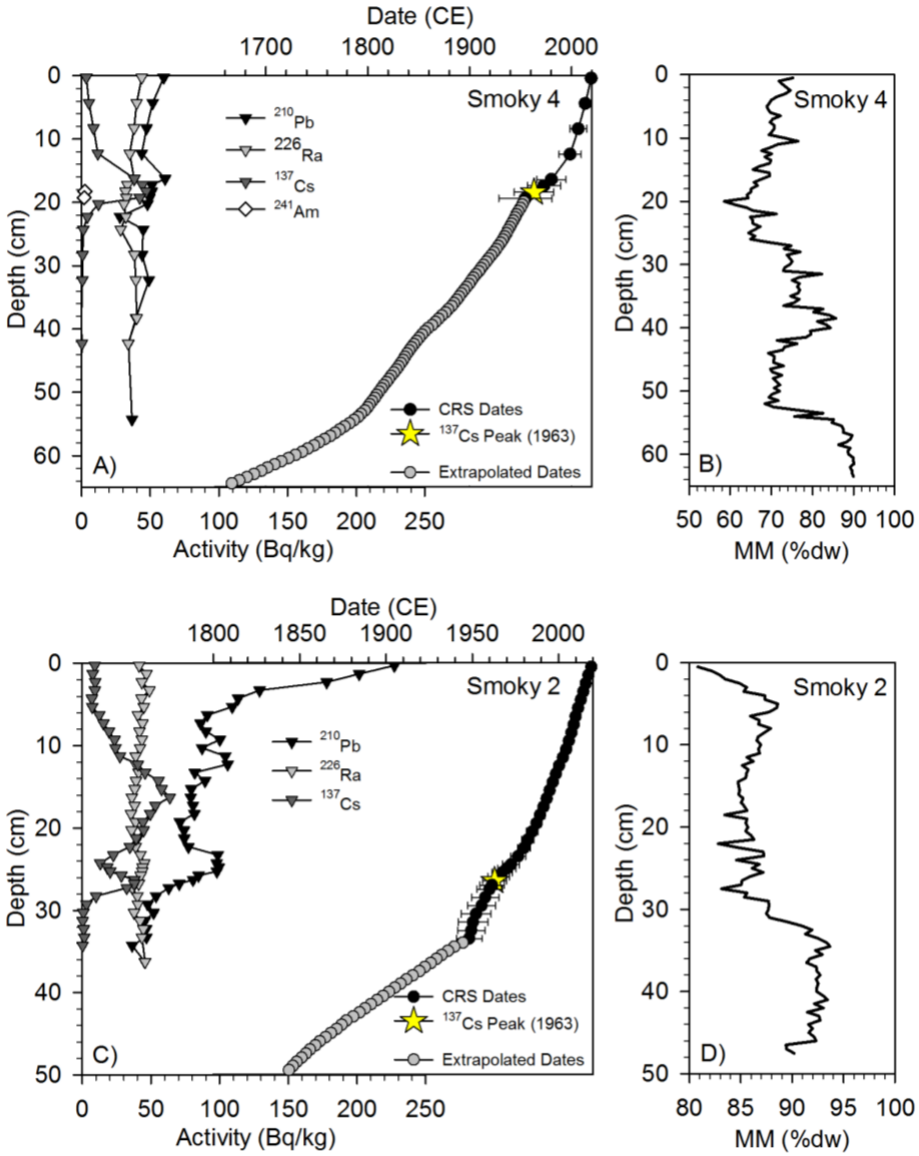

Figure 3.1. Graphs showing results of radiometric dating and LOI analyses. Left panels present activity profiles of ^{210}Pb (black triangles), ^{226}Ra (light grey triangles), ^{137}Cs (dark grey triangles), and ^{241}Am (white diamonds for Smoky 4) for sediment cores from lakes Smoky 4 (A) and Smoky 2 (C). The left panels also present the age-depth relationship (black circles) and extrapolated dates (grey circles) derived from the CRS modelling of the unsupported ^{210}Pb inventories. The ^{137}Cs peaks are indicated by a yellow star. Right panels present carbonate-free mineral matter content (MM) profiles for cores from Smoky 4 (B) and Smoky 2 (D).

The sediment core from Smoky 4 shows little stratigraphic variation in total ^{210}Pb activity and values within the upper 19 cm are only slightly higher than the estimated supported ^{210}Pb activity, as represented by ^{226}Ra activity (Figure 3.1A). Relatively low and constant unsupported

^{210}Pb activity is likely due to dilution from rapid sedimentation at Smoky 4. Inferred rapid sedimentation via input of suspended sediment by floodwaters from the Little Smoky River to this river-proximal lake is consistent with high carbonate-free mineral matter content of the sediment (59-90% of dry mass) (Figure 3.1B). One exception to this is a discernible rise in total ^{210}Pb activity between 14 and 20 cm, including a peak (61 Bq/kg) at 16.5 cm which corresponds to the interval with lowest mineral matter content (58.6%). Background ^{210}Pb activity was reached at 19.5 cm when total ^{210}Pb activity was equal to the estimated supported ^{210}Pb (49 Bq/kg). The ^{137}Cs activity peak (47 Bq/kg) at 18.5 cm is assumed to mark the peak in atmospheric fallout of ^{137}Cs in 1963 and is used as a reference date to constrain the CRS age model. Americium (^{241}Am), another isotope associated with nuclear fallout, was detected in only two samples of this core and they correspond with the peak in ^{137}Cs. Americium is known to be far less mobile than ^{137}Cs and although it was released in lower quantities, it is considered a more trustworthy nuclear fallout marker for 1963 in lake sediment profiles (Appleby et al., 1991). Further, the ^{137}Cs activity peak occurs in the middle of an interval of relatively consistent and low mineral matter content, which suggests the peak reflects atmospheric deposition rather than a consequence of varying input of flood-supplied sediment. Linear extrapolation of the CRS model estimates a basal date of 1666 for the 64.5-cm long core at Smoky 4.

Total ^{210}Pb activity at Smoky 2 is highest at the top of the core (227 Bq/kg) and declines rapidly with depth through the upper 7 cm to 88 Bq/kg (Figure 3.1C). Between 7 and 33 cm, total ^{210}Pb activity declines more gradually, except for distinctive small peaks evident at 12.5 cm (106 Bq/kg) and 25 cm (99 Bq/kg). Background ^{210}Pb was reached at 33.5 cm when total ^{210}Pb activity became equivalent to the estimated supported ^{210}Pb (^{226}Ra) at 46 Bq/kg. This coincided with a downcore increase in mineral matter content from 81 to 94% of sediment dry mass, which

is interpreted to be caused by a shift to greater influx of fluvial sediment that diluted the unsupported ^{210}Pb activity (Figure 3.1D). The ^{137}Cs activity profile at Smoky 2 illustrates two distinct peaks, one at 26.5 cm and the other at 16 cm. The smaller peak in ^{137}Cs activity at 26.5 cm (38 Bq/kg) is assumed to be the peak in atmospheric fallout at 1963 and is used as a reference date to constrain the CRS age model, as was done for the core from Smoky 4. Consistent with this, the first detection of ^{137}Cs activity in this core at 29.5 cm corresponds with an estimated CRS date of 1956 and aligns well with the expected onset of global nuclear fallout in 1954. The second peak in ^{137}Cs activity corresponds to an estimated CRS date of 1993. This peak is likely the outcome of post-depositional remobilization of cesium by local forest fires and, possibly, also some fallout from the Chernobyl nuclear reactor accident in 1986 (Taylor et al., 1988). From the beginning of the second rise at ~23 cm (1978) to its maximum at 16 cm (~1993), there were 23 fires in the Grande Prairie Forest Area that exceeded 40 hectares in size (Government of Alberta, 2021). Forest fires can redistribute ^{137}Cs previously bound to organic matter such as trees, leaf litter and the upper O-horizon of soils, as smoke or ash, which can be redeposited or transported to other surface soils and ultimately deposited into lake basins by runoff (Paliouris et al., 1995). Linear extrapolation of the CRS model estimates a basal date of 1843 for the 49.5-cm long core obtained from Smoky 2.

Of note are the seemingly counterintuitive ^{137}Cs peak depths measured in the two cores. The deeper depth of the 1963 ^{137}Cs peak at Smoky 2 versus Smoky 4 can be reconciled by differences in the focusing factors estimated from the total excess inventories, following methods by Muir et al. (2009; pg. 4804). The focusing factor at Smoky 4 core is 0.2 and signifies the core was obtained from a location where sediment is laterally redistributed towards other portions of

the lake bottom. In comparison, the focusing factor for the Smoky 2 core is 1.3, indicating a more typical mid-lake depositional environment.

3.2 Principal component analysis of elemental composition

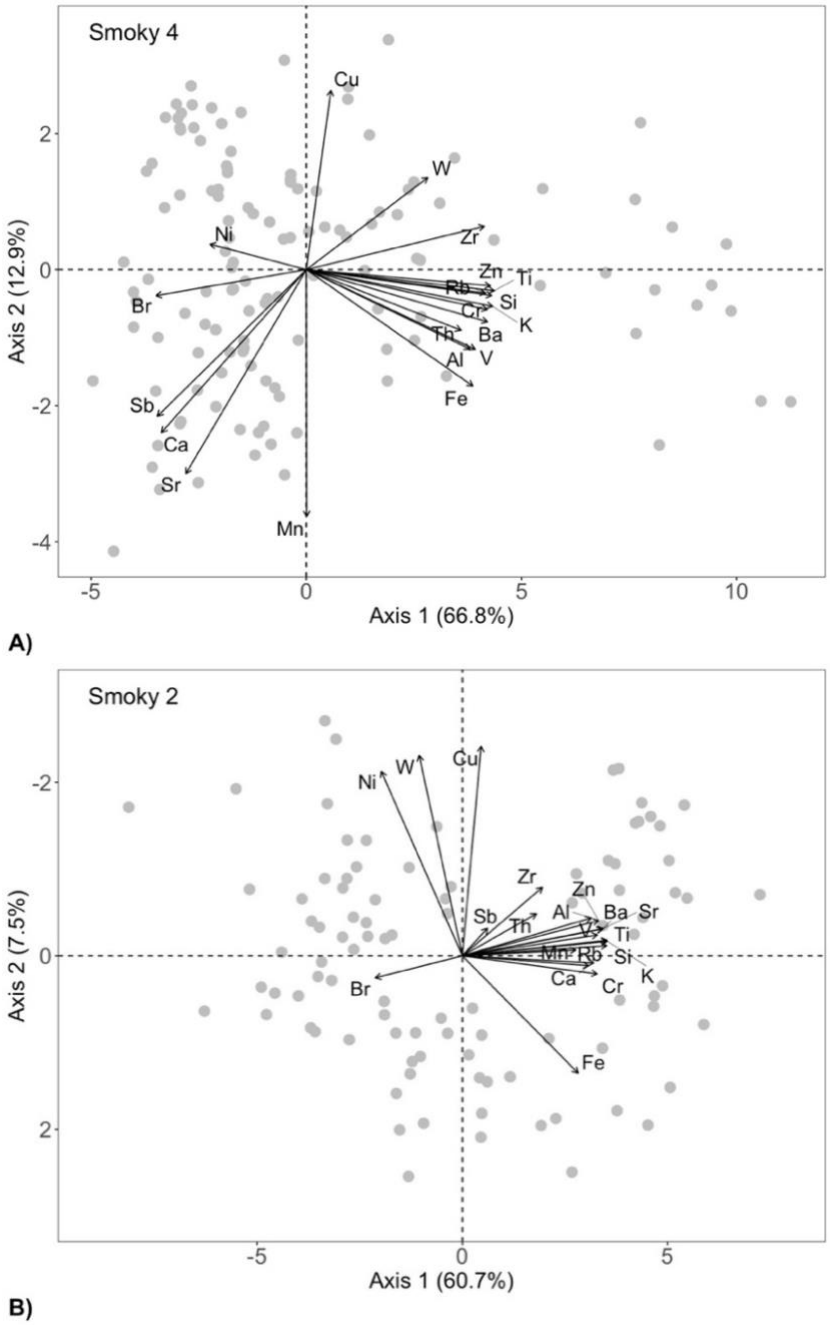

Figure 3.2. Graphs displaying the results of principal component analysis (PCA) on elemental composition of individual sediment intervals obtained from XRF analysis of the sediment cores from lakes Smoky 4 (A) and Smoky 2 (B). Values in brackets next to axis labels indicate the percentage of total variation captured. Vectors represent scores for the 20 active elements included in each PCA.

PCA analyses were conducted on concentrations of 20 elements determined by XRF analysis of the sediment cores from Smoky 4 and Smoky 2 to gain an understanding of the source and composition of sediment deposited in these lakes. At Smoky 4, the first two axes capture 79.7% of the total variation in element concentrations (Figure 3.2A). The first axis captures 66.8% of the variation and is positively correlated with several terrigenous elements (Al, Si, Ti, Rb, Zr, K and Th) that are abundant in mineral-rich sediment (Elghonimy & Sonnenberg, 2021). Axis 1 is negatively correlated with concentrations of Br and Ni, elements that are often associated with more organic-rich sediment (Rapuc et al., 2019). Axis 2 captures considerably less variation than axis 1 (12.9%) and is positively correlated with Cu concentration and negatively correlated with Mn concentration. Concentrations of these elements in sediments are regulated by redox conditions wherein Mn precipitates under oxic conditions and Cu precipitates once conditions become suboxic (Boyle, 2001; Moreno et al., 2008; Elghonimy & Sonnenberg, 2021). Vectors for concentrations of Ca and Sr plot in the lower left quadrant, orthogonal to the terrigenous elements. The distinct grouping of these carbonate-associated elements suggests that the carbonate content in Smoky 4 is endogenic in origin, derived from precipitation in the water column under conditions of evaporative water loss and/or high lake-water pH caused by rising primary production (Boyle, 2001; Lu et al., 2017).

For Smoky 2, the first two PCA axes capture 68.2% of the total variation in concentrations of the 20 elements measured by XRF and show mostly similar patterns of distribution to the PCA of Smoky 4 (Figure 3.2B). Axis 1 captures 60.7% of the variation and, similar to Smoky 4, is positively correlated with several terrigenous elements (including Al, Si, Ti, Rb, Zr, K and Th) and negatively correlated with Br. Axis 2 captures 7.5% of the variation and is negatively correlated with elements regulated by redox conditions, including Cu and Ni

(Elghonimy & Sonnenberg, 2021). Unlike at Smoky 4, vectors for carbonate-associated elements (Ca and Sr) are positively correlated with axis 1 and with the terrigenous elements, indicating that carbonate content in Smoky 2 is detrital in origin. Given the high total variation explained by PCA axis 1 at both lakes and its positive correlation with concentrations of terrigenous elements in both cases, stratigraphic variation in axis 1 scores were used to reconstruct past variation in flood influence at lakes Smoky 4 and Smoky 2.

3.3 Zonation of multi-proxy stratigraphic records

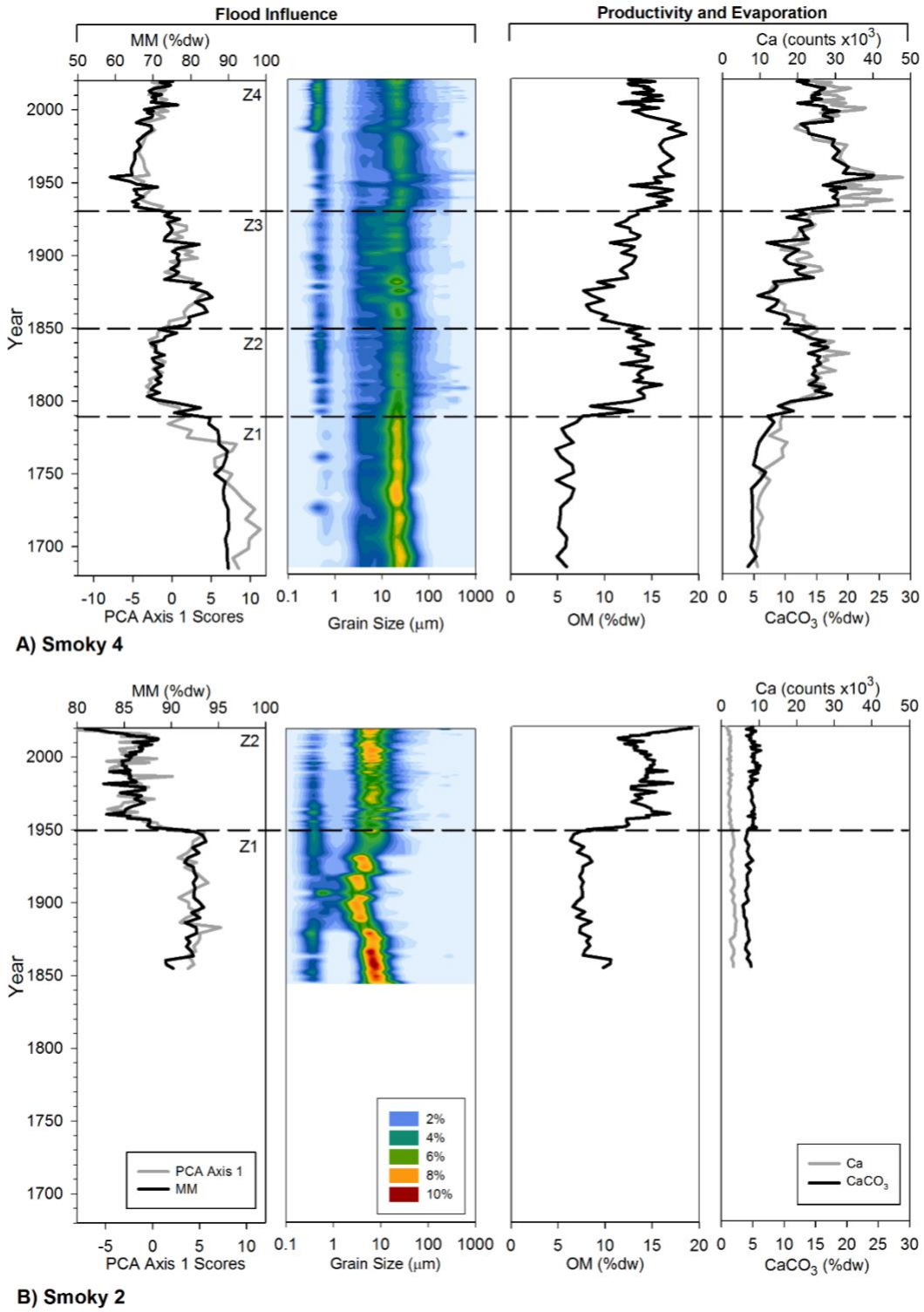

Figure 3.3. Graphs comparing stratigraphic profiles of carbonate-free mineral matter content (MM, black), PCA axis 1 scores (grey), grain size (surface plots), organic matter content (OM, black), calcium carbonate content ($CaCO_3$, black), and calcium concentration (Ca, grey) for Smoky 4 (A) and Smoky 2 (B). Horizontal dashed lines represent boundaries between zones of distinctly different inferred flood influence.

Stratigraphic variation in several of the sedimentary variables analyzed in the cores from Smoky 4 and Smoky 2 allows for delineation of distinctive zones, or time periods, of different hydro-limnological conditions during the past ~150-350 years (Figure 3.3). Stratigraphic profiles of mineral matter content, PCA axis 1 scores and grain size composition are used to inform on temporal variation in the relative influence of flooding whereas relative concentrations of organic matter, calcium carbonate, and calcium inform about past variation of in-lake productivity and evaporation. Zones with relatively high mineral matter content, high PCA axis 1 scores and large grain sizes are interpreted as periods strongly influenced by flooding from the Little Smoky River, as high energy floodwaters deposit allochthonous, larger-grained, inorganic sediment particles rich in terrigenous elements to the lake bottoms (Wolfe et al., 2006). Conversely, intervals of lower mineral matter content, lower PCA axis 1 scores and smaller grain sizes are interpreted as periods of weaker flood influence from the Little Smoky River due to greater relative supply of fine-grained sediment from catchment runoff and in-lake production under conditions of lower energy (Wolfe et al., 2006). Under these hydrological conditions, relatively high concentrations of organic matter (OM; Smoky 4, 2), calcium carbonate ($CaCO_3$; Smoky 4) and calcium (Ca; Smoky 4) are indicative of greater influence of evaporation on lake water balance and higher aquatic primary production. These processes lead to higher ionic content and lake-water pH, which promote precipitation of endogenic carbonates (Boyle, 2001; Cohen, 2003). Based on visual qualitative assessment of stratigraphic variations in the six sedimentary variables shown in Figure 3.3, four zones were identified at Smoky 4 and two zones at Smoky 2. Assuming that sedimentation has been continuous throughout the period captured by the cores and that sill elevation of the oxbow lakes has not varied substantially over time, the ages

associated with the zone boundaries can be used to identify the timing of shifts between weaker and stronger flood influence.

The earliest zone in the Smoky 4 core (Zone 1; ~1680-1790) is characterized by relatively high and consistent mineral matter content (mean = 88%) and PCA axis 1 scores, and the largest grain sizes of the entire record. During this zone, medium silt (15.5 - 31 μm) was the dominant size class and accounted for >10% of the grain-size composition. Relatively low content of calcium carbonate (mean = 6%), organic matter (mean = 6%) and calcium (mean = 12,400 counts) also characterized Zone 1. These results identify that Zone 1 captures an interval of strong flood influence. Zone 2 (~1790-1850) is characterized by marked decline of mineral matter content (mean = 72%), PCA axis 1 scores and relative abundance of medium silt, and an increase in the proportion of clay-sized particles (0-3.9 μm). This is coincident with a doubling of organic matter content (mean = 14%), calcium carbonate (mean = 14%) and Ca (25,400 counts) content. These changes are interpreted as a shift to weaker flood influence, and correspondingly greater evaporation and aquatic productivity. Zone 3 (~1850-1930) is delineated by marked rises in mineral matter content and PCA axis 1 scores, and an abundance of medium-silt sized grains which increased slightly in proportion in this zone. Additionally, organic matter, calcium carbonate content and Ca concentration declined during Zone 3. These changes are interpreted as a shift to stronger influence of flooding. A discernible peak in mineral matter content (max = 86%), PCA axis 1 scores, and a shift to a larger grain size class (~7% medium silt) occurs during the first three decades (~1850-1880) of Zone 3, with coincident declines in relative concentration of organic matter (min = 8%), calcium carbonate (min = 6%) and Ca (min = 12,300 counts). Values during these three decades are comparable to those in Zone 1 and identify an interval of distinctly stronger flood influence compared to the subsequent decades of

Zone 3. Zone 4 (~1930-2019), the most recent period, is characterized by marked declines in mineral matter content and PCA axis 1 scores, a shift to a smaller grain size class, and increases in the content of organic matter, calcium carbonate, and calcium. Most notably, the first five decades (~1930-1980) of this zone capture the lowest mineral matter content (mean = 65%) and PCA axis 1 scores, and the highest content of organic matter (mean = 16%), calcium carbonate (mean = 16%), and calcium (35,600 counts) of the entire ~350-year record. This 50-year period is interpreted as having the lowest flood influence and highest degree of evaporation and productivity of the record from Smoky 4. After ~1980, grain size shifts towards greater proportion of clay-sized particles (<1μm) and the other five indices returned to levels resembling those in Zone 2, demonstrating a slightly stronger influence of flooding in the latter four decades of Zone 4.

At Smoky 2, sediments deposited during Zone 1 (~1860-1950) are characterized by relatively high mineral matter content (mean = 92%) and PCA axis 1 scores, low organic matter content (mean = 8%), and a dominance (8-10%) of fine silt (7.8-15.6 μm) with some smaller, clay-sized particles (~4%). This ~90-year period is interpreted as strongly influenced by river floodwaters. Zone 2 (~1950-2019) is characterized by an abrupt and marked decline in mineral matter content (mean = 86%) and PCA axis 1 scores, and a rise in organic matter content (mean = 14%). These changes support the interpretation of relatively weaker flood influence during Zone 2. The relative content of clay-sized particles declined after the late 1960s, however, and the proportion of medium silt increased, which potentially runs counter to inference of a reduction in flood influence. Beginning at about 1990, a discernible rise in mineral matter content and decline in organic matter content suggest a brief period of increased flood influence within Zone 2. The sharp increase in organic matter from 11 to 19% in the last decade of Zone 2

may represent incomplete diagenesis of recently deposited material. This inference is supported by the high proportion of medium silt that persists during the most recent 10 years of Zone 2. At Smoky 2, the relative content of calcium carbonate (3.4-6.3%) and calcium (1,300-3,900 counts) are substantially lower and less variable than at Smoky 4, and they do not covary with stratigraphic variation in organic and mineral matter content, PCA axis 1 scores, or grain size at Smoky 2. These features suggest that calcium carbonate and Ca in sediments at Smoky 2 are largely sourced from allochthonous input of detrital sediment by river floodwaters, as also indicated in the PCA for the latter (Figure 3.2), but these measurements appear to not be sensitive to variations in influence of river floodwater.

Chapter 4 – Discussion

4.1. Reconstruction of past flood regimes in the Smoky River watershed

Ice-jam flooding is the result of a combination of environmental factors including sufficient snowpack, rate of snowmelt, and the strength and thickness of ice-cover, and plays an important role for recharging ecologically important perched basins at the PAD (Prowse & Lalonde, 1996; Prowse & Conly, 1998; Lamontagne et al., 2021). Long temporal datasets are required to disentangle the roles of natural processes and anthropogenic activities on flood regimes at the PAD, knowledge that is critical for guiding effective natural resource decisions and policies. Here, paleolimnological analyses of sediment records from two oxbow lakes adjacent to the Little Smoky River were used to determine past variation in flood influence within the Smoky River watershed, a key tributary that contributes to ice-jam flood occurrence at the PAD.

Similar to other paleolimnological investigations that have reconstructed flood events (Peng et al., 2005; Wolfe et al., 2006; Parris et al., 2010; Lu et al., 2017; Rapuc et al., 2019), a multi-proxy approach was employed and included analyses of sediment composition by loss-on-ignition (LOI), particle size analysis, and x-ray fluorescence (XRF). Some studies have also used analyses of organic carbon and nitrogen concentrations and their stable isotope ratios as well as magnetic susceptibility to inform interpretations of variations in flooding (Zolitschka, 1998; Meyers & Lallier-Vergès, 1999; Brown et al., 2000; Wolfe et al., 2006). The results of this study show strongly coherent variations in sediment composition (LOI), elemental concentrations (XRF) and grain size at both river-proximal oxbow lakes in the Smoky River watershed, which allowed for the establishment of lake-specific stratigraphic zones to distinguish intervals of stronger and weaker flood influence. Zones consisting of relatively high mineral matter content,

high concentrations of several terrigenous elements (Al, Si, Ti, Rb, Zr, K, Th) as reflected by high PCA axis 1 scores, and large grain sizes were interpreted as intervals when the lakes were strongly influenced by flooding from the Little Smoky River. In contrast, zones with relatively low values of these variables and metrics were interpreted to reflect sediment deposited during intervals of weaker flood influence. As detailed below, the concurrence in directional change of the multiple measurements, the marked differences of values between the zones of inferred stronger and weaker flood influence, and the strong correspondence in timing of zone boundaries between the two oxbow lake records provide confidence in the reconstruction of temporal variation in flood influence for the Smoky River watershed.

Temporal correspondence of the records of flood influence between Smoky 2 and Smoky 4 is evident from comparison of the mineral matter content and PCA axis 1 profiles (Figure 4.1A). The sediment core from Smoky 4 captured more time (~340 years) than the core from Smoky 2 (~160 years), however the timing and direction of change in flood influence is similar at both lakes. Corresponding intervals of stronger and weaker flood influence will herein be referred to as ‘phases’. Using the zone boundaries established for Smoky 4 (Figure 3.3A), four phases were identified: two intervals of stronger flood influence (Phase 1 from ~1680-1790 and Phase 3 from ~1850-1930) and two intervals of weaker flood influence (Phase 2 from ~1790-1850 and Phase 4 from ~1930-2019) (Figure 4.1) The shorter record from Smoky 2 captured the most recent phases, 3 and 4. Smoky 4 appears to transition to Phase 4 around 1930, some 20 years earlier than Smoky 2. Discrepancies between dates estimated for the start of Phase 4 at Smoky 2 and Smoky 4 may be explained by differences in sill elevation. For instance, a higher sill elevation at Smoky 4 would require larger discharge events on the Little Smoky River for floodwaters to reach its basin, such that relatively lower river levels during the period of 1930-

1950 could still inundate Smoky 2 while weak flood influence occurs at Smoky 4. It is also important to note that there is greater error in the dates estimated for the core from Smoky 4 than there is for the core from Smoky 2, and in general, the error associated with CRS dates increases with core depth. For example, the estimated date of ~1930 for the Smoky 4 transition into Phase 4 has an error of >26 years, which overlaps with the Smoky 2 transition at about 1950 (±8.6 years).

Other minor differences between the two Smoky oxbow lakes include their relative susceptibility to flooding. Phase 4 captures the least amount of river floodwater influence in the reconstructions for both lakes, characterized by the lowest mineral matter content and PCA axis 1 scores of their respective cores (Figure 4.1A). However, unlike at Smoky 2, Smoky 4 is also characterized by the highest calcium carbonate and calcium contents of the stratigraphic record during this phase, indicating the presence of endogenic carbonates (Figure 4.1A). Endogenic carbonates typically precipitate in a water column under conditions of greater evaporation and higher aquatic productivity (Boyle, 2001), suggesting Smoky 4 experienced weaker flood influence than Smoky 2 during the past ~90 years. In support of this interpretation, Smoky 4 was also found to have a higher pH (7.14), higher conductivity (328) and lower turbidity (1.88) than Smoky 2 (pH = 6.99; specific conductivity = 188 µS/cm; turbidity = 3.74 FNU). These findings, in addition to the detection of endogenic carbonates at Smoky 4, suggest that this lake has been more productive than Smoky 2 in recent decades and thus has experienced less flooding. Despite differences in susceptibility to river flooding between the lakes, strong temporal correspondence of the records during the past ~160 years suggests the paleolimnological analyses provide a coherent reconstruction of flood influence at the Smoky River watershed. Given that river sediment is most likely delivered to oxbow lakes during high spring discharge events, it is

reasonable to infer the multi-proxy records of flood influence reflect past variation in spring discharge in the Smoky River watershed. The relationship between paleolimnological reconstructions of spring discharge from the 'trigger tributaries' (Smoky and Wabasca River watersheds) and ice-jam flooding at the PAD can now be assessed, and in particular the notion that flood frequency has been in decline since the early 20th century as a result of climate change (Wolfe et al., 2006, 2020).

4.2 Relations between past variation in spring discharge at the upstream trigger tributaries and flood regimes at the PAD

Records of inferred river floodwater influence from oxbow lakes within the Wabasca River watershed (WAB 2; Figure 4.1B) and at the PAD (PAD 15; Figure 4.1C) show similar temporal variations in intervals of stronger and weaker flood influence, which are consistent with the four phases established for the oxbow lakes in the Smoky River watershed (Figure 4.1). The flood record from oxbow lake WAB 2 was constructed in a similar manner as the records from Smoky 2 and Smoky 4 using loss-on-ignition, x-ray fluorescence and grain size (Girard, MSc in progress). This lake is located adjacent to the unregulated Wabasca River ~40 km from its terminus at the confluence with the Peace River. PAD 15 is an oxbow lake adjacent to the Revillon Coupé in the PAD, near its confluence with the Peace River, and its laminated sediments have provided a high-resolution reconstruction of flood frequency and magnitude using measurements of magnetic susceptibility (Wolfe et al., 2006). Phase 1 (~1680-1790) is captured in all three of the stratigraphic records that extend into the 18th century (Smoky 4, WAB 2, and PAD 15). However, there is a clear divergence in the relative flood influence of each lake during this phase. Prior to ~1780, PAD 15 illustrates weak flood influence that gradually strengthens and ultimately peaks around 1800. A similar pattern is detected in the shorter WAB 2

core, whereas the Smoky 4 core demonstrates consistently strong flood influence from the bottom of the core until ~1790. This could be an indication that Smoky 4 was connected to the Little Smoky River at this time or that river levels were closer to the sill elevation of Smoky 4 leading to greater flood susceptibility. Phase 2 (~1790-1850) is captured by the stratigraphic records from the same three lakes and is interpreted as a ~60-year period of weaker flood influence. Phase 3 (~1850-1930) is clearly depicted in all four stratigraphic records and is inferred as a period of stronger flood influence. During this phase, the Smoky 2 record demonstrates consistently strong flood influence for the entire ~80-year period while the WAB 2 stratigraphic record illustrates increasing flood influence. The Smoky 4 and PAD 15 records begin this phase with the strongest flood influence of their respective cores and a gradual decline is inferred since ~1880. The final and most recent interval, Phase 4 (~1930-2019), is interpreted as a period of weaker flood influence across all lakes. For the stratigraphic records of Smoky 4 and PAD 15, this period of weaker flood influence is a continuation of Phase 3 while at WAB 2 and more evidently at Smoky 2, there is a marked decline in relative flood influence at the start of Phase 4.

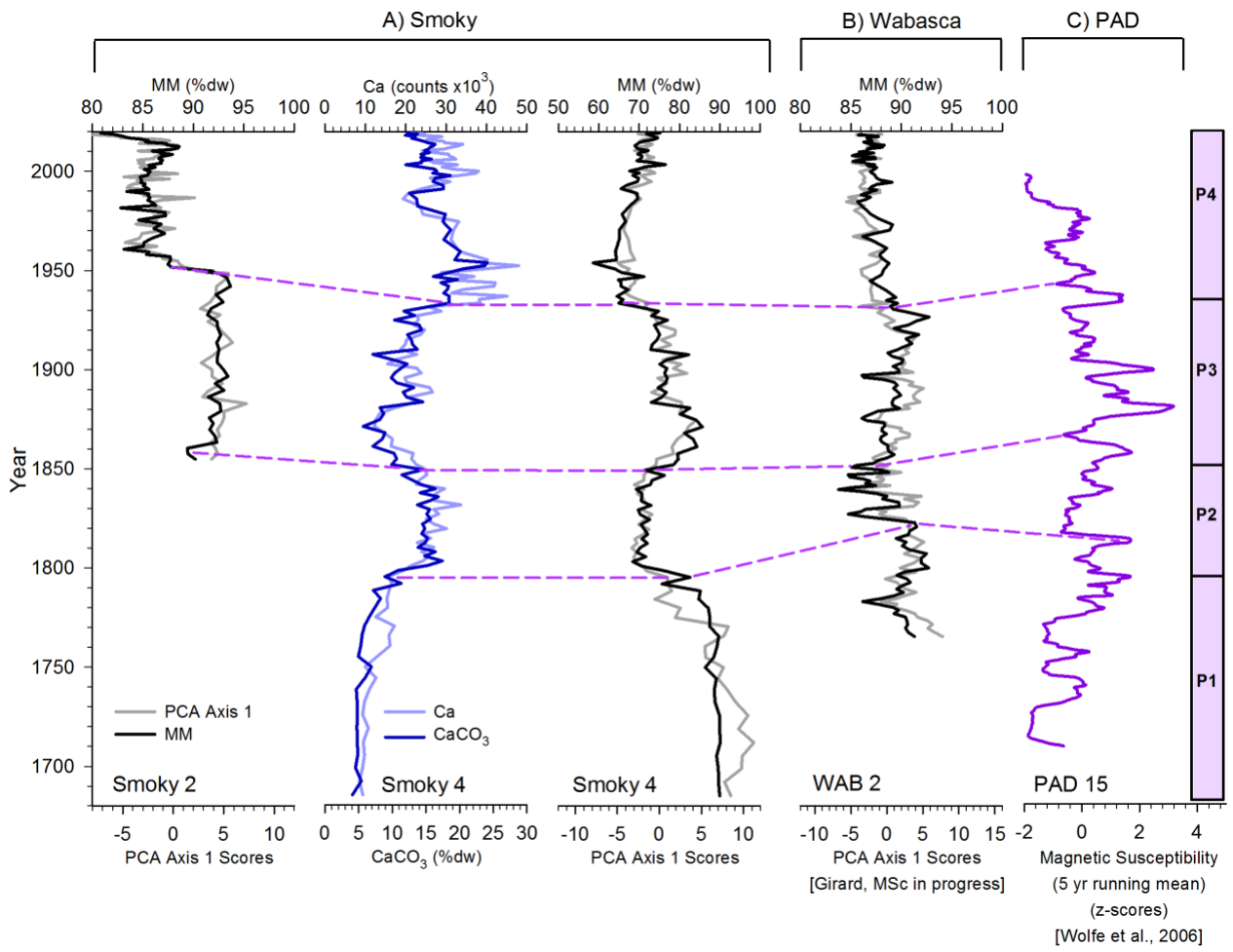

Figure 4.1. Comparison of stratigraphic records from oxbow lakes in the Smoky (A) and Wabasca (B) river watersheds and at the PAD (C). Stratigraphic profiles from lakes in the trigger tributaries (Smoky 2, Smoky 4, WAB 2 [Girard, MSc in progress]) use mineral matter content (MM, black), PCA axis 1 scores (grey), calcium carbonate content ($CaCO_3$, dark blue), and calcium concentration (Ca, light blue) while the flood record from the oxbow lake at the PAD (PAD15; Wolfe et al., 2006) uses magnetic susceptibility (purple). Purple dashed lines represent phase boundaries and were used to visually compare periods of similar flood influence among records. Phases (P1-4) are indicated on the right in purple with black lines denoting the timing of phase shifts established for Smoky 4.

Discrepancies in the timing of phase transitions at each of the four lakes are likely the result of chronological uncertainties. For example, the Phase 2 boundary at Smoky 4 is identified at ~1790 whereas the transition is estimated to occur ~25 years later at PAD 15 (~1815) and ~30 years later at WAB 2 (~1820). This is likely due to greater error in age estimations, which tends to increase with core depth. However, confidence in the Smoky 4 core chronology is strengthened by use of the Reference Date Method, which constrains the excess ^{210}Pb inventory and improves age estimations. Even though the focusing factor estimated for the Smoky 4 core is

well below 1, there appears to be little evidence of abrupt shifts in the mineral matter content and PCA axis 1 scores of the XRF data to suggest there are gaps in the stratigraphic record. At PAD 15, the core chronology relied exclusively on a linear sedimentation rate based on the ^{137}Cs profile and was constrained by a ^{14}C measurement at the base of the record. Thus, differences between the estimated dates for PAD 15 and the Smoky and Wabasca oxbow lakes are not unexpected. Even with these discrepancies between estimated ages of the phase transitions, the similarities in directional change among lakes from independent watersheds separated by up to 840 km of river length is striking. Given this distance between sites and the different tributaries supplying floodwaters, it suggests that climate serves an overriding influence on flood regimes at the Smoky River watershed, Wabasca River watershed, and the Peace River at the PAD.

4.3 The role of climate on Smoky River spring discharge and ice-jam flooding at the PAD

Consistent timing and direction of changes in inferred flood influence at lakes in the trigger tributaries and downstream at the PAD do not indicate a weakening of flood influence coincident with the construction of the W.A.C. Bennett Dam in 1968. Rather, they indicate a decline in flood influence that began in the early- to mid-1900s. Indeed, more than 200 years of close correspondence in phases of strong and weak flood influence suggest that occurrence of ice-jam flooding at the PAD has long been dependent on spring discharge from upstream unregulated tributaries and their contribution to dynamic ice breakup on the Peace River. It has been postulated that the reduction in snowpack volume in the Smoky River watershed from 1976-1996, associated with a change in atmospheric circulation patterns (Keller, 1997; Romolo et al., 2006), resulted in lower spring discharge and was at least partially responsible for declining ice-jam flood events in the PAD. However, a shift to weaker flood influence at ~1976 was not evident in either of the Smoky oxbow lake flood records, but instead a more substantial

shift was detected at ~1930-1950. Others assert, based on hydrometric records which identify greater winter flows on the Peace River since regulation in 1968, that increased freeze-up levels on the Peace River are the cause for decreased ice-jam flooding at the PAD (Prowse & Conly, 1998; Beltaos et al., 2006; Beltaos, 2014). However, there is no evidence of directional change coincident with 1968 in the PAD 15 flood record. The most recent phase of weak flood influence identified at all lakes across three watersheds and 840 km of river distance is consistent with widespread concerns of reduced flood frequency and lake drying at the PAD, yet all records indicate this trend began several decades before regulation by the W.A.C. Bennett Dam, as do paleolimnological records of perched basin water balance in the PAD (Wolfe et al., 2020). The timing of the most recent directional change to weaker flood influence identified at both Smoky oxbow lakes is closely aligned with analysis of historical drought records by Asong et al. (2018). Their study found that the foothills of the Rocky Mountains have been subject to declining trends in Standardized Precipitation Evapotranspiration Index (SPEI) with moisture deficits from 1950 to 2013 with extremely dry conditions occurring during the early 1960s, 1980s, early 1990s and 2000s. These trends are in agreement with the most recent interval (Phase 4; ~1930-2019) among all oxbow lakes which depicts a shift to reduced flood influence from ~1930-1950 until the early 2000s when a slight increase in flood influence is detected. This strongly suggests the influence of climate as a broad regional-scale driver affecting spring discharge and flood regimes across all three watersheds.

Chapter 5 – Conclusions, Implications and Recommendations

5.1 Key findings and relevance of research

Multi-proxy analysis of sediment cores from two oxbow lakes adjacent to the Little Smoky River were used to reconstruct a flood history and infer temporal variation of spring discharge for the Smoky River watershed during the past ~160-340 years. Coherent stratigraphic variation in several physical and geochemical variables provided multiple lines of evidence for robust interpretation of flood influence at this watershed. Flood records for Smoky 2 and Smoky 4 captured two and four zones of alternating strength in flood influence, respectively. The two zones at Smoky 2 correspond to the direction and timing of flood influence changes captured in most recent two zones at Smoky 4, spanning the past ~160 years. Close alignment between the two records provides confidence in the methods and flood reconstructions. A comparison of four paleolimnological flood records of oxbow lakes in the Smoky River watershed, Wabasca River watershed, and at the Peace-Athabasca Delta revealed four broadly coincident phases of alternating weak and strong flood influence since the late 1700s. Comparable temporal patterns of change in the flood regimes of oxbow lakes adjacent to unregulated tributaries and in the regulated lower Peace River region emphasize the importance of spring discharge from upstream tributaries on the ice-jam flood regime at the PAD and regional climate as the common driver of hydrological change. A common recent interval of weak flood influence found at all four oxbow lakes aligns with concerns of a drying delta expressed by local Indigenous Peoples and past scientific research. However, results from this study identify the shift to weaker flood influence began in the early- to mid-1900s in the Smoky River watershed, which is consistent with the most recent drying trend interpreted from lake sediment cores downstream in the Wabasca River watershed and at the PAD, providing further evidence of climate as the dominant driver of

change rather than regulation beginning in 1968 by the W.A.C. Bennett Dam. Despite changing Peace River flows and higher freeze-up levels in the post-regulation period emphasized in other studies (Beltaos et al., 2006; Beltaos, 2014, 2019), our findings suggest climate has played a substantial and unifying role in controlling flood regime shifts at the PAD by regulating spring discharge at upstream tributaries and their ability to trigger ice-jam flood events at the PAD.

Spring discharge from upstream tributaries, most notably the Smoky and Wabasca rivers, has long been known to play an influential role in triggering ice-jam floods capable of inundating perched lakes at the PAD (Prowse & Conly, 1998; Peters & Prowse, 2006). Common variation in relative flood influence during the past ~300 years and consistencies in the timing and direction of hydrological changes across all oxbow lakes suggests climate-driven changes in spring discharge is the main driver. This is critical new information that contributes to the Wood Buffalo National Park Action Plan and specifically efforts to improve baseline data to inform decision making related to the hydrological integrity of the PAD. With nearly $90 million already invested since 2012 and $60 million more pledged as of December 2020 (Pruys, 2021), it is pertinent to direct funding into strategies that will be effective against the changes induced by climate rather than ways in which to mitigate the effects of river regulation, if this is a desirable outcome.

5.2 Future recommendations

To strengthen the new knowledge generated in this study, it is recommended to obtain sediment cores from additional oxbow lakes in the Smoky River watershed. Unfortunately, it does not appear possible to acquire sediment core records of flood influence along the main Smoky River channel as river-proximal lakes were not found using Google Earth. However, additional oxbow lakes along the Little Smoky River could be sampled to further test for

reproducibility and increase confidence in the timing of directional change established by the two oxbow lakes examined in this study. Smoky 1 and 3, oxbow lakes which were cored in September 2019 along with Smoky 2 and 4, are unlikely to provide informative stratigraphic records of flood influence in the Smoky River watershed as loss-on-ignition results indicated they were either too flood-prone or not sufficiently flood-prone. Furthermore, a deeper understanding of the relationship between local climate and spring discharge at the Smoky River watershed may be gleaned by ongoing reconstruction of temporal variation in water balance of closed-drainage lakes in the Smoky sub-basin (Thibault, MSc in progress). Here, dry conditions at closed-drainage lakes coincident with periods of weak flood influence at oxbow lakes in the Smoky River watershed would provide additional evidence of climate controls on spring discharge.

The mineral matter content, grain size measurements, and XRF elemental composition of lake sediment used in this study provide a robust basis of assessing temporal variation in flood influence at oxbow lakes. Methods could easily be expanded in future studies to include magnetic susceptibility as an additional proxy for river floodwater influence by simply taking measurements on the same Itrax-XRF core scanner used for XRF analysis. Alternatively, mass specific magnetic susceptibility could be measured using a known volume of sample and a Bartington MS2B sensor following methods by Dearing (1994) to avoid inaccuracies resulting from the varying air space between sediment samples and the core-scanner in the previous method. Principal component analysis of XRF data is becoming increasingly used in paleoenvironmental studies (Elghonimy & Sonnenberg, 2021; Peti & Augustinus, 2022) and was an effective method in this study for identifying terrigenous elements correlated with axis 1 and used as an indicator of floodwater influence at the oxbow lakes. However, more information

regarding flood energy or intensity could be gleaned by exploring the elements correlated with axis 2. Lastly, it is recommended that a more thorough exploration of grain size be conducted to identify the sources of sediment contributing to the two distinct modes illustrated in Figure 3.3 using an End Member Modelling approach (e.g., Parris et al., 2010). This would require additional sample collection to characterize relevant end members including suspended river sediment and lake catchment sediment. This methodology could identify the relative contribution of each sediment source to differentiate between local catchment runoff and river floodwater deposits.

The paleolimnological reconstruction of flood histories generated by this study infer past spring discharge for the Smoky River watershed and supplement the limited hydrometric data available. The long-term perspective that the results of this study provide can be used as a basis for future research in areas such as climate modelling and future flow scenarios of the Smoky River, which would be useful for identifying impending challenges that will need to be addressed by government and natural resource agencies to ensure effective stewardship of the PAD.

References

Appleby, P. G. (2001). Chronostratigraphic techniques in recent sediments. In W. M. Last & J. P. Smol (Eds.), *Tracking Environmental Change Using Lake Sediments: Basin Analysis, Coring, and Chronological Techniques, Developments in Paleoenvironmental Research, Vol. 1* (pp. 171–203). Kluwer Academic Publishers.

Appleby, P. G., Richardson, N., & Nolan, P. J. (1991). ^{241}Am dating of lake sediments. *Hydrobiologia*, *214*(1), 35–42. https://doi.org/10.1007/BF00050929

Asong, Z. E., Wheater, H. S., Bonsal, B., Razavi, S., & Kurkute, S. (2018). Historical drought patterns over Canada and their teleconnections with large-scale climate signals. *Hydrology and Earth System Sciences*, *22*(6), 3105–3124. https://doi.org/10.5194/hess-22-3105-2018

Beierle, B. D., Lamoureux, S. F., Cockburn, J. M. H., & Spooner, I. (2002). A new method for visualizing sediment particle size distributions. *Journal of Paleolimnology*, *27*(2), 279–283. https://doi.org/10.1023/A:1014209120642

Beltaos, S. (2014). Comparing the impacts of regulation and climate on ice-jam flooding of the Peace-Athabasca Delta. *Cold Regions Science and Technology*, *108*, 49–58. https://doi.org/10.1016/j.coldregions.2014.08.006

Beltaos, S. (2018). Frequency of ice-jam flooding of Peace-Athabasca Delta. *Canadian Journal of Civil Engineering*, *45*(1), 71–75. https://doi.org/10.1139/cjce-2017-0434

Beltaos, S. (2019). Ice-jam flood regime of the Peace-Athabasca Delta: Update in light of the 2014 event. *Cold Regions Science and Technology*, *165*, 102791. https://doi.org/10.1016/j.coldregions.2019.102791

Beltaos, S., & Peters, D. L. (2020). Naturalized flow regime of the regulated Peace River, Canada, during the spring breakup of the ice cover. *Cold Regions Science and Technology*, *172*, 103005. https://doi.org/10.1016/j.coldregions.2020.103005

Beltaos, S., & Peters, D. L. (2021). Naturalizing the freezeup regimes of regulated rivers and exploring implications to spring ice-jam flooding. *Hydrological Processes*, *35*(8), e14321. https://doi.org/10.1002/HYP.14321

Beltaos, S., Prowse, T. D., & Carter, T. (2006). Ice regime of the lower Peace River and ice-jam flooding of the Peace-Athabasca Delta. *Hydrological Processes*, *20*(19), 4009–4029. https://doi.org/10.1002/hyp.6417

Boyle, J. F. (2001). Inorganic geochemical methods in paleolimnology. In W. M. Last & J. P. Smol (Eds.), *Developments in Paleoenvironmental Research. Tracking Environmental Change Using Lake Sediments, Vol. 2* (pp. 83–142). Kluwer Academic Publishers.

Brown, S. L., Bierman, P. R., Lini, A., & Southon, J. (2000). 10 000 yr record of extreme hydrologic events. *Geology*, *28*(4), 335–338. https://doi.org/10.1130/0091-7613(2000)028%3C0335:YROEHE%3E2.3.CO;2

Campbell, C. (1998). Late Holocene Lake Sedimentology and Climate Change in Southern Alberta, Canada. *Quaternary Research*, *49*(1), 96–101. https://doi.org/10.1006/qres.1997.1946

Cohen, A. S. (2003). Sedimentological Archives in Lake Deposits. In *Paleolimnology: History and Evolution of Lake Systems* (pp. 162–207). Oxford University Press.

Davies, S. J., Lamb, H. F., & Roberts, S. J. (2015). Micro-XRF Core Scanning in Palaeolimnology: Recent Developments. In *Micro-XRF Studies of Sediment Cores* (Vol. 17, pp. 189–226). Springer, Dordrecht. https://doi.org/10.1007/978-94-017-9849-5_7

Dean, W. E. (1974). Determination of carbonate and organic matter in calcareous sediments and sedimentary rocks by loss on ignition: comparison with other methods. *Journal of Sedimentary Petrology*, *44*(1), 242–248. https://doi.org/10.1306/74d729d2-2b21-11d7-8648000102c1865d

Dearing, J. (1994). *Environmental Magnetic Susceptibility: Using the Bartington MS2 System* (pp. 10-14). Bartington Instruments. https://gmw.com/wp-content/uploads/2019/03/JDearing-Handbook-OM0409.pdf

Dudgeon, D., Arthington, A. H., Gessner, M. O., Kawabata, Z. I., Knowler, D. J., Lévêque, C., Naiman, R. J., Prieur-Richard, A. H., Soto, D., Stiassny, M. L. J., & Sullivan, C. A. (2006). Freshwater biodiversity: Importance, threats, status and conservation challenges. In *Biological Reviews of the Cambridge Philosophical Society* (Vol. 81, Issue 2, pp. 163–182). https://doi.org/10.1017/S1464793105006950

Elghonimy, R., & Sonnenberg, S. (2021, July 26). *A Principal Component Analysis Approach to Understanding Relationships Between Elemental Geochemistry Data and Deposition, Niobrara Formation, Denver Basin, CO* [Paper]. SPE/AAPG/SEG Unconventional

Resources Technology Conference (URTeC), Houston, Texas, USA. https://doi.org/10.15530/urtec-2021-5440

Girard, C. (2022). *Paleohydrology of the Wabasca River and relations with flood regimes at the downstream Peace-Athabasca Delta* [Unpublished Masters Thesis]. University of Waterloo.

Government of Alberta. (2021, September 16). *Historical Wildfire Database: Alberta wildfire records*. https://wildfire.alberta.ca/resources/historical-data/historical-wildfire-database.aspx

Gregory, B. R. B., Reinhardt, E. G., Macumber, A. L., Nasser, N. A., Patterson, R. T., Kovacs, S. E., & Galloway, J. M. (2017). Sequential sample reservoirs for Itrax-XRF analysis of discrete samples. *Journal of Paleolimnology*, *57*(3), 287–293. https://doi.org/10.1007/s10933-017-9944-4

Hall, R. I., Wolfe, B. B., & Wiklund, J. A. (2019). Discussion of "frequency of ice-jam flooding of peace-athabasca delta." *Canadian Journal of Civil Engineering*, *46*(3), 236–238. https://doi.org/10.1139/CJCE-2018-0407/ASSET/IMAGES/LARGE/CJCE-2018-0407F2.JPEG

Heiri, O., Lotter, A. F., & Lemcke, G. (2001). Loss on ignition as a method for estimating organic and carbonate content in sediments: reproducibility and comparability of results. *Journal of Paleolimnology*, *25*, 101–110. https://doi.org/10.1023/A:1008119611481

Independent Environmental Consultants. (2018). *Strategic Environmental Assessment of Wood Buffalo National Park World Heritage Site*. https://www.pc.gc.ca/en/pn-np/nt/woodbuffalo/info/action/strategie-env-assessment

Kassambara, A., & Mundt, F. (2020). *factoextra: Extract and Visualize the Results of Multivariate Data Analyses* (R package version 1.0.7). https://CRAN.R-project.org/package=factoextra

Kay, M. L., Wiklund, J. A., Remmer, C. R., Neary, L. K., Brown, K., Ghosh, A., MacDonald, E., Thomson, K., Vucic, J. M., Wesenberg, K., Hall, R. I., & Wolfe, B. B. (2019). Bi-directional hydrological changes in perched basins of the Athabasca Delta (Canada) in recent decades caused by natural processes. *Environmental Research Communications*, *1*(8), 081001. https://doi.org/10.1088/2515-7620/ab37e7

Keller, R. (1997). *Variability in spring snowpack and winter atmospheric circulation pattern frequencies in the Peace River Basin* [Masters Thesis]. University of Saskatchewan. HARVEST. https://harvest.usask.ca/handle/10388/etd-06192012-085011

Lamontagne, J. R., Jasek, M., & Smith, J. D. (2021). Coupling physical understanding and statistical modeling to estimate ice jam flood frequency in the northern Peace-Athabasca Delta under climate change.*Cold Regions Science and Technology, 192*, 103383. https://doi.org/10.1016/j.coldregions.2021.103383

Last, W. M. (2001). Mineralogical Analysis of Lake Sediments. In W. M. Last & J. P. Smol (Eds.), *Tracking Environmental Change Using Lake Sediments: Basin Analysis, Coring, and Chronological Techniques, Developments in Paleoenvironmental Research, Vol. 2* (pp. 143–187). Kluwer Academic Publishers. https://doi.org/10.1007/0-306-47670-3_6

Leconte, R., Pietroniro, A., Peters, D. L., & Prowse, T. D. (2001). Effects of flow regulation on hydrologic patterns of a large, inland delta. *Regulated Rivers-Research & Management, 17*, 51–65. https://doi.org/10.1002/1099-1646(200101/02)17:1%3C51::AID-RRR588%3E3.0.CO;2-V

Lincoln, M. (2022). *clipr: Read and Write from the System Clipboard* (R package version 0.8.0). https://CRAN.R-project.org/package=clipr

Lu, Y., Fritz, S. C., Stone, J. R., Krause, T. R., Whitlock, C., Brown, E. T., & Benes, J. v. (2017). Trends in catchment processes and lake evolution during the late-glacial and early- to mid-Holocene inferred from high-resolution XRF data in the Yellowstone region. *Journal of Paleolimnology, 58*(4), 551–569. https://doi.org/10.1007/s10933-017-9991-x

Meyers, P. A., & Lallier-Vergès, E. (1999). Lacustrine Sedimentary Organic Matter Records of Late Quaternary Paleoclimates. *Journal of Paleolimnology 21*, 345–372. https://doi.org/10.1023/A:1008073732192

Mikisew Cree First Nation. (2014). *Petition to the World Heritage Committee: Requesting Inclusion of Wood Buffalo National Park on the List of World Heritage in Danger*. https://cpawsnab.org/wp-content/uploads/2018/03/Mikisew_Petition_respecting_UNESCO_Site_256_-_December_8_2014.pdf

Mikutta, R., Kleber, M., Kaiser, K., & Jahn, R. (2005). Review: Organic matter removal from soils using hydrogen peroxide, sodium hypochlorite, and disodium peroxodisulfate. *Soil Science Society of America Journal*, *69*(1), 120–135. https://doi.org/10.2136/sssaj2005.0120

Moreno, A., Valero-Garcés, B. L., González-Sampériz, P., & Rico, M. (2008). Flood response to rainfall variability during the last 2000 years inferred from the Taravilla Lake record (Central Iberian Range, Spain). *Journal of Paleolimnology*, *40*(3), 943–961. https://doi.org/10.1007/s10933-008-9209-3

Muir, D. C. G., Wang, X., Yang, F., Nguyen, N., Jackson, T. A., Evans, M. S., Douglas, M., Köck, G., Lamoureux, S., Pienitz, R., Smol, J. P., Vincent, W. F., & Dastoor, A. (2009). Spatial trends and historical deposition of mercury in eastern and northern Canada inferred from lake sediment cores. *Environmental Science and Technology*, *43*(13), 4802–4809. https://doi.org/10.1021/ES8035412/SUPPL_FILE/ES8035412_SI_001.PDF

Paliouris, G., Taylor, H. W., Wein, R. W., Svoboda, J., & Mierzynski, B. (1995). Fire as an agent in redistributing fallout ^{137}Cs in the Canadian boreal forest. *Science of The Total Environment*, *160–161*, 153–166. https://doi.org/10.1016/0048-9697(95)04353-3

Parks Canada. (2019). *Wood Buffalo National Park World Heritage Site Action Plan*. https://www.pc.gc.ca/en/pn-np/nt/woodbuffalo/info/action

Parris, A. S., Bierman, P. R., Noren, A. J., Prins, M. A., & Lini, A. (2010). Holocene paleostorms identified by particle size signatures in lake sediments from the northeastern United States. *Journal of Paleolimnology*, *43*(1), 29–49. https://doi.org/10.1007/s10933-009-9311-1

Peace-Athabasca Delta Project Group (PADPG). (1973). *Peace-Athabasca Delta Project, Technical Report and Appendices: Volume 1, Hydrological Investigations; Volume 2, Ecological Investigations*. Peace–Athabasca Delta Project Group, Delta Implementation Committee, Governments of Alberta, Saskatchewan and Canada.

Peace-Athabasca Delta Technical Studies (PADTS). (1996). Final Report. PADTS Steering Committee, Fort Chipewyan, Alberta.

Peng, Y., Xiao, J., Nakamura, T., Liu, B., & Inouchi, Y. (2005). Holocene East Asian monsoonal precipitation pattern revealed by grain-size distribution of core sediments of Daihai Lake in

Inner Mongolia of north-central China. *Earth and Planetary Science Letters*, *233*(3–4), 467–479. https://doi.org/10.1016/j.epsl.2005.02.022

Peters, D. L., & Prowse, T. D. (2001). Regulation effects on the lower Peace River, Canada. *Hydrological Processes*, *15*, 3181–3194. https://doi.org/10.1002/hyp.321

Peters, D. L., & Prowse, T. D. (2006). Generation of streamflow to seasonal high waters in a freshwater delta, northwestern Canada. *Hydrological Processes*, *20*(19), 4173–4196. https://doi.org/10.1002/HYP.6425

Peti, L., & Augustinus, P. C. (2022). Micro-XRF-inferred depositional history of the Orakei maar lake sediment sequence, Auckland, New Zealand. *Journal of Paleolimnology*, *67*, 327–344. https://doi.org/10.1007/s10933-022-00235-y

Pomeroy, J., Shook, K., Fang, X., Brown, T., & Marsh, C. (2013). *Development of a Snowmelt Runoff Model for the Lower Smoky River* [Report No. 13]. Centre for Hydrology, University of Saskatchewan. http://citeseerx.ist.psu.edu/viewdoc/download?doi=10.1.1.705.7915&rep=rep1&type=pdf

Prowse, T. D., & Conly, F. M. (1998). Effects of climatic variability and flow regulation on ice-jam flooding of a northern delta. *Hydrological Processes*, *12*(10-11), 1589–1610. https://doi.org/10.1002/(SICI)1099-1085(199808/09)12:10/11<1589::AID-HYP683>3.0.CO;2-G

Prowse, T. D., & Lalonde, V. (1996). Open-water and ice-jam flooding of a Northern Delta. *Nordic Hydrology*, *27*(1–2), 85–100. https://doi.org/10.2166/nh.1996.0021

Pruys, S. (2021, July 25). *UN again urges Canada to get on with saving Wood Buffalo park*. Cabin Radio. https://cabinradio.ca/68484/news/environment/un-again-urges-canada-to-get-on-with-saving-wood-buffalo-park/

Rapuc, W., Sabatier, P., Arnaud, F., Palumbo, A., Develle, A. L., Reyss, J. L., Augustin, L., Régnier, E., Piccin, A., Chapron, E., Dumoulin, J. P., & von Grafenstein, U. (2019). Holocene-long record of flood frequency in the Southern Alps (Lake Iseo, Italy) under human and climate forcing. *Global and Planetary Change*, *175*, 160–172. https://doi.org/10.1016/j.gloplacha.2019.02.010

Rokaya, P., Peters, D. L., Elshamy, M., Budhathoki, S., & Lindenschmidt, K. (2020). Impacts of future climate on the hydrology of a northern headwaters basin and its implications for a

downstream deltaic ecosystem. *Hydrological Processes*, *34*(7), 1630–1646. https://doi.org/10.1002/hyp.13687

Romolo, L., Prowse, T. D., Blair, D., Bonsal, B. R., Marsh, P., & Martz, L. W. (2006). The synoptic climate controls on hydrology in the upper reaches of the Peace River Basin. Part II: Snow ablation. *Hydrological Processes*, *20*(19), 4113–4129. https://doi.org/10.1002/HYP.6422

Schindler, D. W., & Donahue, W. F. (2006). An impending water crisis in Canada's western prairie provinces. *Proceedings of the National Academy of Sciences (PNAS)*, *103*(19), 7210–7216. https://doi.org/10.1073/pnas.0601568103

Schindler, D. W., Smol, & John P. (2006). Cumulative Effects of Climate Warming and Other Human Activities on Freshwaters of Arctic and Subarctic North America. *AMBIO: A Journal of the Human Environment*, *35*(4), 160–168. https://doi.org/10.1579/0044-7447(2006)35[160:CEOCWA]2.0.CO;2

Schnurrenberger, D., Russell, J., & Kelts, K. (2003). Classification of lacustrine sediments based on sedimentary components. *Journal of Paleolimnology*, *29*, 141–154. https://doi.org/10.1023/A:1023270324800

Sinnatamby, N. R., Yi, Y., Sokal, M. A., Clogg-Wright, K. P., Asada, T., Vardy, S. R., Karst-Riddoch, T. L., Last, W. M., Johnston, J. W., Hall, R. I., Wolfe, B. B., & Edwards, T. W. D. (2010). Historical and paleolimnological evidence for expansion of Lake Athabasca (Canada) during the Little Ice Age. *Journal of Paleolimnology*, *43*, 705–717. https://doi.org/10.1007/s10933-009-9361-4

Taylor, H., Svoboda, J., Henry, G., & Wein, R. (1988). Post-Chernobyl ^{134}Cs and ^{137}Cs Levels at Some Localities in Northern Canada on JSTOR. *Arctic*, *41*(4), 293–296. https://www.jstor.org/stable/40510746?seq=1

Telford, J.V., Kay, M.L., Vander Heide, H., Wiklund, J. A., Owca, T. J., Faber, J. A., Wolfe, B. B., & Hall, R. I. (2021). Building upon open-barrel corer and sectioning systems to foster the continuing legacy of John Glew. *Journal of Paleolimnology 65*, 271–277. https://doi.org/10.1007/s10933-020-00162-w

Thibault, H. (2022). *Reconstructing past variation in lake water balances to identify the role of a shifting hydroclimate at watersheds upstream of the drying Peace-Athabasca Delta*. [Unpublished Masters Thesis]. University of Waterloo.

Timoney, K. P. (2009). Three centuries of change in the Peace–Athabasca Delta, Canada. *Climatic Change, 93,* 485–515. https://doi.org/10.1007/S10584-008-9536-4

UNESCO World Heritage Centre, & International Union for Conservation of Nature. (2017). *Reactive Monitoring Mission to Wood Buffalo National Park, Canada*. https://whc.unesco.org/en/documents/156893

Wickham, H. (2016). *ggplot2: Elegant Graphics for Data Analysis*. Springer-Verlag New York. https://ggplot2.tidyverse.org

Wolfe, B. B., Hall, R. I., Edwards, T. W. D., & Johnston, J. W. (2012). Developing temporal hydroecological perspectives to inform stewardship of a northern floodplain landscape subject to multiple stressors: paleolimnological investigations of the Peace–Athabasca Delta. *Environmental Reviews*, *20*(3), 191–210. https://doi.org/10.1139/a2012-008

Wolfe, B. B., Hall, R. I., Last, W. M., Edwards, T. W. D., English, M. C., Karst-Riddoch, T. L., Paterson, A., & Palmini, R. (2006). Reconstruction of multi-century flood histories from oxbow lake sediments, Peace-Athabasca Delta, Canada. *Hydrological Processes*, *20*(19), 4131–4153. https://doi.org/10.1002/hyp.6423

Wolfe, B. B., Hall, R. I., Wiklund, J. A., & Kay, M. L. (2020). Past variation in Lower Peace River ice-jam flood frequency. *Environmental Reviews*, *28*(3), 209–217. https://doi.org/10.1139/er-2019-0047

Woodward, G., Perkins, D. M., & Brown, L. E. (2010). Climate change and freshwater ecosystems: Impacts across multiple levels of organization. *Philosophical Transactions of the Royal Society B: Biological Sciences*, *365,* 2093–2106. https://doi.org/10.1098/rstb.2010.0055

Zolitschka, B. (1998). A 14,000 year sediment yield record from western Germany based on annually laminated lake sediments. *Geomorphology, 22*(1), 1–17. https://doi.org/10.1016/S0169-555X(97)00051-2

Appendices

Appendix A – Radiometric Dating

Table A.1. Measured ^{210}Pb, ^{137}Cs, ^{226}Ra, and ^{241}Am values (Bq/kg) and CRS dates for the Smoky 4 sediment core. Grey cells represent extrapolated values. Empty cells represent sediment intervals that were not measured. Depths reported are the top measurements of each sediment interval (i.e., depth of 1 cm represents sediment interval 1-1.5 cm).

Depth (cm)	CRS Dates	CRS Error ± 2 sigma	^{210}Pb (Bq/kg)	^{210}Pb error (1 std. dev.)	^{226}Ra (Bq/kg)	^{226}Ra error (1 std. dev.)	^{137}Cs (Bq/kg)	^{137}Cs error (1 std. dev.)	^{241}Am (Bq/kg)	^{241}Am error (1 std. dev.)
0	2019.18	0.67	59.80	8.49	43.80	1.90	3.37	1.29		
0.5	2018.64	1.44								
1	2017.92	2.14								
1.5	2017.22	2.87								
2	2016.43	3.29								
2.5	2015.58	4.06								
3	2014.86	4.44								
3.5	2014.03	4.98								
4	2013.37	5.16	51.70	7.85	40.10	1.76	5.26	1.28		
4.5	2012.52	5.68								
5	2011.74	6.04								
5.5	2010.88	6.59								
6	2010.04	6.89								
6.5	2009.07	7.48								
7	2008.33	7.76								
7.5	2007.50	8.12								
8	2006.66	8.34	47.30	7.82	38.10	1.72	8.63	1.38		
8.5	2005.82	8.67								
9	2004.85	9.01								
9.5	2004.01	9.31								
10	2002.75	9.69								
10.5	2001.76	10.00								
11	2000.65	10.29								
11.5	1999.70	10.53								
12	1998.58	10.78	43.80	6.40	35.00	1.45	11.70	1.35		
12.5	1997.37	11.05								
13	1995.82	11.37								
13.5	1993.89	11.70								
14	1992.13	12.04								
14.5	1990.36	12.34								
15	1987.62	12.81								
15.5	1984.68	13.28								
16	1980.26	14.34	60.70	8.32	38.20	1.74	38.40	3.41		
16.5	1976.44	15.18								
17	1972.94	16.22	51.10	8.29	33.30	1.72	44.30	3.88		
17.5	1968.05	17.43								
18	1963.09	19.32	51.10	8.37	31.90	1.76	46.90	4.08	2.33	0.92
18.5	1956.11	21.73								
19	1954.59	26.03	49.50	6.81	32.60	1.44	42.30	3.60	1.83	0.70
19.5	1953.16									
20	1951.66		47.90	7.64	30.80	1.56	12.30	1.50		
20.5	1949.95									
21	1947.94									
21.5	1945.96									

22	1944.64		27.90	8.31	32.20	1.44	4.09	1.38
22.5	1942.93							
23	1941.24							
23.5	1939.51							
24	1937.72		44.80	6.17	28.40	1.35	1.22	0.94
24.5	1936.26							
25	1934.42							
25.5	1932.73							
26	1930.68							
26.5	1928.18							
27	1926.21							
27.5	1923.73							
28	1921.28		44.00	5.60	38.40	1.34	0.74	0.79
28.5	1918.70							
29	1916.36							
29.5	1913.74							
30	1911.32							
30.5	1908.99							
31	1906.16							
31.5	1903.77							
32	1901.78		49.00	6.43	39.40	1.47	0.63	0.92
32.5	1899.44							
33	1896.96							
33.5	1894.55							
34	1892.02							
34.5	1889.72							
35	1887.36							
35.5	1884.73							
36	1882.38							
36.5	1878.94							
37	1876.36							
37.5	1872.81							
38	1869.54		39.50	7.17	40.00	1.69	-0.14	0.58
38.5	1866.54							
39	1863.29							
39.5	1859.05							
40	1856.10							
40.5	1853.38							
41	1850.56							
41.5	1848.06							
42	1845.36		34.10	6.00	33.80	1.39	0.13	2.35
42.5	1843.10							
43	1840.83							
43.5	1838.62							
44	1836.62							
44.5	1834.76							
45	1832.66							
45.5	1830.44							
46	1828.16							
46.5	1825.74							
47	1823.01							
47.5	1820.76							
48	1818.41							
48.5	1815.72							
49	1813.64							
49.5	1811.24							
50	1808.90							
50.5	1806.92							
51	1804.42							

51.5	1802.02							
52	1799.91							
52.5	1797.14							
53	1793.47							
53.5	1790.51							
54	1786.37		36.60	6.69	0.00	0.00	-0.64	0.73
54.5	1782.15							
55	1777.35							
55.5	1772.61							
56	1768.20							
56.5	1763.32							
57	1757.63							
57.5	1752.22							
58	1747.38							
58.5	1741.24							
59	1735.68							
59.5	1729.05							
60	1722.29							
60.5	1715.32							
61	1708.54							
61.5	1701.81							
62	1695.62							
62.5	1688.50							
63	1681.60							
63.5	1674.05							
64	1666.63							

Table A.2. Measured ^{210}Pb, ^{137}Cs, and ^{226}Ra values (Bq/kg) and CRS dates for the Smoky 2 sediment core. Grey cells represent extrapolated values. Empty cells represent sediment intervals that were not measured. Depths reported are the top measurements of each sediment interval (i.e., depth of 1 cm represents sediment interval 1-1.5 cm).

Depth (cm)	**CRS Dates**	**CRS Error ± 2 sigma**	**^{210}Pb (Bq/kg)**	**^{210}Pb error (1 std. dev.)**	**^{226}Ra (Bq/kg)**	**^{226}Ra error (1 std. dev.)**	**^{137}Cs (Bq/kg)**
0	2019.00	0.12	227.20	14.70	41.30	3.45	9.04
0.5	2018.22	0.23					
1	2017.31	0.29	201.60	12.70	46.60	3.08	7.54
1.5	2016.61	0.35					
2	2015.83	0.40	177.90	9.53	43.30	2.18	9.35
2.5	2015.04	0.47					
3	2014.42	0.51	129.10	9.46	48.80	2.44	9.04
3.5	2013.76	0.58					
4	2012.97	0.63	113.40	7.87	43.10	2.00	6.96
4.5	2012.15	0.71					
5	2011.37	0.77	109.10	8.05	44.70	2.06	7.24
5.5	2010.53	0.86					
6	2009.98	0.90	91.00	8.87	40.40	2.31	12.30
6.5	2009.41	0.96					
7	2008.86	1.00	86.00	8.22	43.80	2.16	15.30
7.5	2008.28	1.05					
8	2007.52	1.11	90.00	8.36	41.60	2.41	19.40
8.5	2006.87	1.17					
9	2006.04	1.23	100.10	7.52	43.30	2.05	23.40
9.5	2005.24	1.30					
10	2004.52	1.36	87.20	9.30	42.00	2.40	24.00
10.5	2003.70	1.43					
11	2002.57	1.52	104.00	9.26	38.80	2.46	27.40

11.5	2001.51	1.61					
12	2000.38	1.71	105.80	8.02	39.10	2.19	40.50
12.5	1999.26	1.81					
13	1998.51	1.87	81.80	7.57	40.90	2.00	45.70
13.5	1997.67	1.95					
14	1996.67	2.04	89.30	7.57	39.00	2.14	55.40
14.5	1995.71	2.13					
15	1994.88	2.21	79.30	7.80	38.10	2.24	57.70
15.5	1994.05	2.29					
16	1993.16	2.38	78.90	9.07	36.00	2.29	63.70
16.5	1992.16	2.47					
17	1991.32	2.56	80.50	8.11	38.00	2.23	53.10
17.5	1990.43	2.65					
18	1989.34	2.77	81.60	9.28	35.30	2.39	49.40
18.5	1988.08	2.89					
19	1987.30	2.98	71.00	8.06	38.60	2.26	44.10
19.5	1986.14	3.09					
20	1984.73	3.24	73.90	9.46	35.90	2.48	44.60
20.5	1983.52	3.36					
21	1982.23	3.51	74.20	7.80	40.00	2.21	39.20
21.5	1981.02	3.64					
22	1980.04	3.77	77.30	8.97	38.80	2.48	34.60
22.5	1978.54	3.96					
23	1976.57	4.25	98.60	7.36	42.20	2.90	22.50
23.5	1974.39	4.57					
24	1972.43	4.89	97.80	8.54	45.20	2.78	13.00
24.5	1970.02	5.31	99.30	8.26	43.90	2.12	18.10
25	1967.30	5.82	98.00	8.76	43.60	2.43	20.20
25.5	1965.23	6.24	84.60	7.86	42.50	2.18	28.40
26	1962.96	6.73	80.60	8.31	37.50	2.28	37.90
26.5	1961.48	7.08	70.50	6.76	41.10	1.91	37.80
27	1960.01	7.41	62.90	8.55	36.40	2.43	32.30
27.5	1958.56	7.65					
28	1957.47	7.87	53.70	7.75	40.00	2.11	10.00
28.5	1956.43	7.97					
29	1955.46	8.11	47.50	5.92	40.50	1.80	2.96
29.5	1954.12	8.24					
30	1952.25	8.65	51.90	6.36	37.70	1.88	0.72
30.5	1951.09	8.67					
31	1950.42	8.61	45.40	5.88	42.00	1.79	0.15
31.5	1949.87	8.18					
32	1949.44	7.93	46.40	6.20	44.40	1.85	1.00
32.5	1948.95	7.56					
33	1948.20	7.39	46.60	5.41	43.30	1.67	1.39
33.5	1944.56						
34	1939.60		36.30	5.62			0.21
34.5	1935.97						
35	1932.25						
35.5	1929.27						
36	1925.92		45.40	5.83	45.70	1.76	
36.5	1922.56						
37	1919.41						
37.5	1915.47						
38	1911.86						
38.5	1908.46						
39	1905.11						
39.5	1901.79						
40	1898.40						
40.5	1894.85						

41	1891.33	
41.5	1887.82	
42	1884.75	
42.5	1881.02	
43	1877.08	
43.5	1874.32	
44	1871.46	
44.5	1868.17	
45	1865.02	
45.5	1861.62	
46	1859.08	
46.5	1855.97	
47	1853.64	
47.5	1851.10	
48	1848.26	
48.5	1846.04	
49	1843.85	

Appendix B – Loss-on-Ignition

Table B.1. Measured loss-on-ignition values for sediment dry weight, water content (%H2O), organic matter content (%OM), mineral matter content (%MM; including and excluding carbonates), and carbonate content (%CaCO3) at lake Smoky 4. Depths reported are the top measurements of each sediment interval (i.e., depth of 1 cm represents sediment interval 1-1.5 cm).

Depth (cm)	Total interval dry weight (g)	%H_20 (g/g wet wt.)	%OM (% dry wt.)	%MM (+$CaCO_3$) (% dry wt.)	%MM (-$CaCO_3$) (% dry wt.)	%$CaCO_3$ (% dry wt.)
0	3.83	88.70	12.55	87.45	75.20	12.25
0.5	4.18	84.56	14.43	85.57	71.84	13.72
1	5.63	83.11	15.35	84.65	72.72	11.92
1.5	5.59	83.06	12.88	87.12	73.70	13.42
2	6.42	78.08	12.53	87.47	74.61	12.86
2.5	6.93	79.54	12.74	87.26	73.44	13.81
3	6.08	80.26	14.13	85.87	71.21	14.67
3.5	7.08	79.85	14.70	85.30	70.01	15.28
4	5.72	79.54	14.18	85.82	69.47	16.35
4.5	7.43	77.41	14.98	85.02	68.94	16.08
5	6.82	78.16	15.22	84.78	69.24	15.54
5.5	7.54	76.82	14.81	85.19	69.82	15.37
6	7.30	75.60	12.98	87.02	72.24	14.78
6.5	8.50	76.51	14.14	85.86	70.33	15.53
7	6.49	78.37	16.07	83.93	69.68	14.24
7.5	7.24	75.87	14.67	85.33	70.67	14.66
8	7.45	76.57	15.10	84.90	70.71	14.19
8.5	7.25	76.48	14.01	85.99	70.18	15.81
9	8.10	76.09	16.22	83.78	69.46	14.32
9.5	6.95	74.87	12.34	87.66	73.33	14.33
10	10.14	71.46	11.52	88.48	76.50	11.98
10.5	7.72	76.84	14.24	85.76	71.55	14.22
11	8.40	74.55	13.95	86.05	69.79	16.26
11.5	7.05	74.95	15.77	84.23	67.63	16.60
12	8.08	74.85	13.94	86.06	70.06	16.00
12.5	7.37	73.98	12.98	87.02	68.43	18.59
13	7.92	76.25	13.77	86.23	69.89	16.34
13.5	8.29	74.01	14.36	85.64	69.57	16.07
14	6.31	78.27	15.53	84.47	66.96	17.52
14.5	5.37	80.83	16.87	83.13	65.53	17.59
15	6.95	78.26	18.02	81.98	69.47	12.51
15.5	6.16	80.13	16.78	83.22	69.63	13.59
16	7.44	78.67	18.64	81.36	67.58	13.78
16.5	6.35	78.49	16.33	83.67	65.81	17.86
17	5.86	79.24	15.86	84.14	66.65	17.49
17.5	6.92	78.91	16.26	83.74	65.10	18.64
18	5.79	78.73	17.31	82.69	65.06	17.63
18.5	7.19	76.19	15.80	84.20	64.11	20.09
19	6.75	79.31	16.35	83.65	64.38	19.27
19.5	6.38	78.05	17.36	82.64	58.56	24.08
20	6.64	78.35	15.30	84.70	61.00	23.70
20.5	7.62	74.94	15.44	84.56	63.99	20.57
21	8.89	74.08	16.02	83.98	65.61	18.37
21.5	8.82	71.77	12.72	87.28	71.21	16.08
22	5.85	79.39	15.45	84.55	64.88	19.67
22.5	7.61	76.65	17.27	82.73	65.54	17.19
23	7.50	77.11	16.15	83.85	65.50	18.35

23.5	7.67	74.44	14.55	85.45	67.28	18.17
24	7.96	76.23	16.49	83.51	65.89	17.62
24.5	6.48	77.43	17.09	82.91	64.48	18.43
25	8.17	75.74	15.58	84.42	66.04	18.38
25.5	7.53	73.27	16.56	83.44	64.96	18.48
26	9.07	72.85	14.94	85.06	69.57	15.49
26.5	11.13	67.58	13.46	86.54	74.83	11.71
27	8.72	69.99	13.58	86.42	73.08	13.34
27.5	11.03	65.55	12.68	87.32	77.02	10.31
28	10.89	69.52	12.26	87.74	73.78	13.96
28.5	11.45	65.97	11.17	88.83	74.49	14.34
29	10.39	68.23	12.69	87.31	75.07	12.24
29.5	11.65	68.59	12.75	87.25	74.44	12.81
30	10.74	67.54	13.78	86.22	73.21	13.01
30.5	10.34	69.16	13.36	86.64	72.92	13.72
31	12.57	63.19	10.62	89.38	82.27	7.10
31.5	10.63	68.75	13.18	86.82	76.86	9.97
32	8.81	71.23	12.69	87.31	75.11	12.20
32.5	10.39	68.99	11.81	88.19	76.87	11.32
33	11.02	67.20	13.34	86.66	76.33	10.33
33.5	10.70	66.76	13.18	86.82	76.97	9.85
34	11.23	65.92	12.90	87.10	76.51	10.60
34.5	10.19	68.38	12.09	87.91	74.71	13.20
35	10.48	68.37	11.64	88.36	76.76	11.59
35.5	11.72	66.50	12.32	87.68	75.58	12.11
36	10.41	69.92	12.46	87.54	73.01	14.53
36.5	15.28	57.50	9.25	90.75	82.60	8.15
37	11.44	66.61	11.02	88.98	80.24	8.73
37.5	15.79	55.10	7.76	92.24	84.13	8.11
38	14.50	60.30	8.67	91.33	85.67	5.66
38.5	13.34	64.77	9.89	90.11	81.19	8.92
39	14.41	56.99	8.06	91.94	83.41	8.52
39.5	18.82	50.41	8.52	91.48	84.37	7.11
40	13.10	61.07	10.26	89.74	79.49	10.25
40.5	12.08	62.04	9.69	90.31	79.69	10.63
41	12.54	65.22	11.65	88.35	78.44	9.90
41.5	11.08	68.23	14.04	85.96	71.38	14.58
42	12.01	65.69	12.31	87.69	76.29	11.40
42.5	10.02	67.79	13.82	86.18	73.27	12.91
43	10.10	69.50	13.08	86.92	72.76	14.16
43.5	9.81	71.42	14.31	85.69	69.32	16.38
44	8.89	70.23	15.19	84.81	70.71	14.11
44.5	8.29	72.77	12.53	87.47	70.65	16.82
45	9.29	71.17	13.89	86.11	70.54	15.58
45.5	9.86	71.01	13.31	86.69	72.99	13.70
46	10.13	67.39	14.68	85.32	69.77	15.54
46.5	10.76	69.00	14.59	85.41	70.31	15.10
47	12.12	68.15	11.73	88.27	72.60	15.67
47.5	10.01	68.24	15.07	84.93	70.45	14.49
48	10.41	68.89	13.92	86.08	71.26	14.82
48.5	11.94	67.02	13.52	86.48	72.13	14.36
49	9.25	70.30	14.05	85.95	70.71	15.24
49.5	10.65	69.34	13.10	86.90	72.03	14.87
50	10.39	70.40	16.06	83.94	70.13	13.81
50.5	8.79	70.61	14.16	85.84	69.45	16.39
51	11.08	68.27	13.53	86.47	71.68	14.79
51.5	10.69	69.39	14.17	85.83	68.42	17.41
52	9.35	69.28	14.22	85.78	70.54	15.23
52.5	12.33	64.23	12.72	87.28	76.39	10.89

53	16.30	54.83	8.51	91.49	82.59	8.91
53.5	13.14	64.81	13.02	86.98	75.66	11.32
54	18.38	51.80	7.66	92.34	85.16	7.18
54.5	18.74	51.19	7.00	93.00	84.76	8.24
55	21.34	45.18	5.45	94.55	87.13	7.41
55.5	21.04	48.34	5.91	94.09	87.52	6.57
56	19.58	46.20	6.67	93.33	87.48	5.85
56.5	21.68	42.46	4.81	95.19	89.69	5.50
57	25.26	39.38	5.37	94.63	89.32	5.32
57.5	24.01	41.27	6.56	93.44	88.49	4.95
58	21.49	50.22	6.73	93.27	86.37	6.90
58.5	27.28	39.22	4.87	95.13	89.17	5.96
59	24.69	37.83	6.75	93.25	88.62	4.63
59.5	29.44	35.19	6.43	93.57	88.82	4.75
60	30.05	33.91	5.31	94.69	89.90	4.79
60.5	30.95	34.87	5.29	94.71	89.97	4.74
61	30.08	35.69	5.10	94.90	90.11	4.80
61.5	29.91	35.98	5.97	94.03	89.18	4.85
62	27.46	39.10	5.86	94.14	89.61	4.53
62.5	31.64	32.37	4.94	95.06	89.67	5.39
63	30.65	33.40	5.96	94.04	89.97	4.07
63.5	33.52	29.80	5.10	94.90	90.31	4.59
64	32.96	32.97	5.71	94.29	90.32	3.97

Table B.2. Measured loss-on-ignition values for sediment dry weight, water content (%H2O), organic matter content (%OM), mineral matter content (%MM; including and excluding carbonates), and carbonate content (%CaCO3) at lake Smoky 2. Depths reported are the top measurements of each sediment interval (i.e., depth of 1 cm represents sediment interval 1-1.5 cm).

Depth (cm)	Total interval dry weight (g)	%H_20 (g/g wet wt.)	%OM (% dry wt.)	%MM (+$CaCO_3$) (% dry wt.)	%MM (-$CaCO_3$) (% dry wt.)	%$CaCO_3$ (% dry wt.)
0	2.99	93.54	19.19	80.81	75.78	5.03
0.5	3.57	89.24	17.86	82.14	77.29	4.86
1	4.49	85.89	17.05	82.95	78.96	3.99
1.5	3.61	87.73	16.51	83.49	78.27	5.21
2	4.22	86.22	15.17	84.83	79.33	5.50
2.5	5.32	83.11	14.43	85.57	80.80	4.76
3	5.33	83.34	14.72	85.28	80.31	4.97
3.5	6.03	80.45	12.67	87.33	82.48	4.85
4	7.45	73.71	12.65	87.35	83.32	4.03
4.5	7.91	70.59	11.41	88.59	84.15	4.43
5	7.64	74.90	11.51	88.49	83.78	4.70
5.5	9.07	69.25	12.23	87.77	83.29	4.47
6	6.56	77.84	14.08	85.92	81.33	4.59
6.5	7.31	75.86	13.20	86.80	81.94	4.86
7	7.55	75.71	13.28	86.72	81.40	5.32
7.5	7.43	72.52	12.08	87.92	83.10	4.82
8	8.75	74.78	12.71	87.29	82.27	5.01
8.5	6.78	78.27	13.30	86.70	81.46	5.24
9	7.87	74.66	13.44	86.56	80.44	6.12
9.5	8.21	74.05	13.05	86.95	82.23	4.71
10	8.13	75.77	13.30	86.70	81.40	5.31
10.5	7.50	76.58	13.18	86.82	81.96	4.86
11	8.38	74.08	14.41	85.59	79.27	6.32
11.5	7.53	75.46	13.79	86.21	80.55	5.66
12	7.59	76.89	14.87	85.13	80.13	5.00
12.5	9.32	72.10	14.28	85.72	80.44	5.29

13	7.74	76.09	14.47	85.53	80.73	4.81
13.5	7.68	74.19	14.51	85.49	80.21	5.28
14	7.97	76.30	15.27	84.73	79.60	5.13
14.5	8.16	75.54	15.20	84.80	79.60	5.21
15	7.67	74.75	15.11	84.89	79.89	5.00
15.5	7.32	75.45	15.23	84.77	79.03	5.74
16	7.45	77.68	14.78	85.22	79.77	5.45
16.5	8.20	75.89	14.97	85.03	78.81	6.22
17	6.66	77.15	14.66	85.34	79.83	5.51
17.5	6.67	77.94	14.39	85.61	79.58	6.03
18	7.48	76.96	16.59	83.41	77.52	5.90
18.5	9.99	72.58	14.42	85.58	81.19	4.39
19	7.21	75.23	14.51	85.49	79.65	5.84
19.5	9.55	73.25	14.31	85.69	80.59	5.10
20	10.29	70.88	14.53	85.47	80.81	4.66
20.5	8.98	70.71	14.01	85.99	81.20	4.79
21	9.71	69.75	13.72	86.28	80.57	5.72
21.5	8.25	74.64	17.20	82.80	78.22	4.58
22	6.08	77.12	15.23	84.77	79.80	4.97
22.5	7.39	76.19	12.82	87.18	82.36	4.82
23	7.59	76.98	12.77	87.23	82.89	4.34
23.5	8.17	76.07	15.44	84.56	79.88	4.69
24	7.14	77.40	13.19	86.81	81.96	4.85
24.5	7.75	76.34	13.91	86.09	81.13	4.97
25	8.25	75.22	12.84	87.16	82.38	4.78
25.5	7.53	76.30	14.12	85.88	80.80	5.08
26	7.56	76.19	14.88	85.12	79.84	5.27
26.5	6.79	79.02	14.96	85.04	79.84	5.19
27	7.15	78.90	16.89	83.11	78.29	4.82
27.5	9.27	74.73	14.40	85.60	80.25	5.35
28	9.39	70.05	14.67	85.33	81.06	4.27
28.5	12.03	62.43	12.31	87.69	82.31	5.38
29	15.25	61.18	12.27	87.73	82.63	5.10
29.5	14.15	59.10	12.31	87.69	82.67	5.02
30	13.41	60.30	12.53	87.47	82.36	5.10
30.5	14.83	56.60	12.18	87.82	82.90	4.92
31	18.36	53.61	10.54	89.46	84.10	5.36
31.5	19.08	49.37	9.05	90.95	85.35	5.60
32	19.38	46.69	8.07	91.93	87.52	4.41
32.5	16.79	48.98	8.73	91.27	86.86	4.40
33	20.25	44.86	7.49	92.51	88.33	4.18
33.5	23.49	41.88	6.69	93.31	89.17	4.14
34	31.98	41.28	6.32	93.68	89.88	3.80
34.5	23.42	45.78	7.74	92.26	87.85	4.40
35	24.02	44.11	7.07	92.93	88.80	4.13
35.5	19.21	48.03	8.27	91.73	87.36	4.37
36	21.57	48.23	8.61	91.39	86.38	5.01
36.5	21.72	45.08	7.66	92.34	88.37	3.97
37	20.31	46.43	7.60	92.40	87.76	4.64
37.5	25.44	43.10	7.29	92.71	88.65	4.05
38	23.25	45.67	7.69	92.31	88.15	4.16
38.5	21.94	45.81	7.47	92.53	88.26	4.27
39	21.65	45.77	7.60	92.40	88.52	3.87
39.5	21.41	45.75	7.62	92.38	88.35	4.03
40	21.83	44.92	7.02	92.98	88.65	4.33
40.5	22.92	41.74	6.57	93.43	90.00	3.43
41	22.70	46.26	7.85	92.15	88.56	3.59
41.5	22.66	44.60	6.97	93.03	89.41	3.62
42	19.80	48.19	8.53	91.47	87.44	4.03

42.5	24.04	44.22	7.39	92.61	88.67	3.95
43	25.45	45.24	7.28	92.72	88.50	4.21
43.5	17.78	49.30	8.43	91.57	87.28	4.29
44	18.49	47.89	8.03	91.97	87.50	4.47
44.5	21.20	47.97	8.39	91.61	87.65	3.96
45	20.32	46.20	7.87	92.13	88.27	3.86
45.5	21.95	47.44	7.67	92.33	87.89	4.43
46	16.42	53.99	10.61	89.39	85.29	4.10
46.5	20.00	54.31	10.55	89.45	84.82	4.63
47	15.03	54.81	9.82	90.18	85.43	4.75
47.5	16.39	54.66	9.71	90.29	85.95	4.34
48	18.37	53.66	9.47	90.53	85.77	4.76
48.5	14.29	62.93	12.62	87.38	81.99	5.39
49	14.10	60.42	12.53	87.47	82.17	5.30

Appendix C – Particle Size Analysis

Table C.1. Wentworth particle size classification showing proportion of particles from each sediment interval of the Smoky 4 core within each category. Categories include clay (4-2 and <2 µm), very fine silt (8-4 µm), fine silt (16-8 µm), medium silt (31-16 µm), coarse silt (63-31 µm), very fine sand (125-63 µm), fine sand (250-125 µm), medium sand (500-250 µm), coarse sand (>500 µm). Also included are the mean, median, and mode for each sediment interval. Cells with dashes represent samples lost during processing. Depths reported are the top measurements of each sediment interval (i.e., depth of 1 cm represents sediment interval 1-1.5 cm).

Depth (cm)	Median (µm)	Mean (µm)	Mode (µm)	>500 µm (%)	500-250 µm (%)	250-125 µm (%)	125-63 µm (%)	63-31 µm (%)	31-16 µm (%)	16-8 µm (%)	8-4 µm (%)	4-2 µm (%)	<2 µm (%)
0	11.21	20.30	18.66	0.00	0.11	1.90	4.53	11.42	21.75	17.48	10.97	7.45	24.40
0.5	10.90	21.05	18.63	0.00	0.12	2.23	5.03	11.16	20.63	17.47	11.38	7.67	24.32
1	11.72	22.89	18.64	0.00	0.18	2.91	5.20	11.44	21.11	17.61	11.51	7.78	22.26
1.5	12.15	25.28	18.67	0.00	0.59	3.50	5.48	11.59	20.98	16.64	10.84	7.94	22.44
2	9.03	20.11	18.63	0.00	0.17	2.42	4.42	10.08	19.00	16.19	10.95	7.39	29.38
2.5	9.43	22.06	18.61	0.00	0.19	3.17	5.22	9.99	18.41	16.22	11.12	7.29	28.40
3	8.52	23.52	0.41	0.00	0.67	3.68	4.98	9.16	16.96	15.73	11.19	7.17	30.45
3.5	12.34	36.02	21.22	0.00	3.35	4.41	6.17	11.13	18.54	14.16	9.37	7.05	25.82
4	10.17	26.40	0.42	0.00	0.78	4.45	5.75	10.28	18.11	14.80	9.88	7.36	28.59
4.5	6.99	22.98	0.37	0.00	0.63	3.50	5.66	9.28	14.54	14.05	10.87	6.85	34.63
5	11.66	42.90	18.67	0.78	4.41	3.76	5.35	10.35	17.80	14.11	9.53	7.35	26.57
5.5	9.31	25.47	0.41	0.00	0.74	4.19	5.66	9.90	17.23	15.00	10.56	7.48	29.24
6	9.65	24.14	18.61	0.00	0.59	3.65	5.41	9.95	17.99	16.09	11.48	7.81	27.04
6.5	10.60	25.87	18.62	0.00	0.67	4.06	5.99	10.58	18.39	15.69	10.62	7.26	26.74
7	10.22	37.22	0.41	0.66	3.39	3.12	5.41	10.07	17.10	14.56	10.12	7.28	28.30
7.5	9.33	25.37	0.41	0.00	0.63	4.12	6.01	10.12	16.91	15.07	11.23	7.93	27.98
8	11.36	46.30	18.64	1.62	4.03	3.77	5.42	9.91	17.15	14.38	10.00	7.50	26.22
8.5	10.52	26.16	18.64	0.00	0.69	4.17	5.98	10.74	18.20	15.39	10.79	7.74	26.30
9	10.78	25.79	18.65	0.00	0.56	3.90	6.43	11.22	18.32	15.13	10.54	7.62	26.28
9.5	11.76	38.22	18.66	0.60	3.43	3.42	5.52	10.74	18.49	15.17	10.28	7.95	24.39
10	14.03	32.09	10.82	0.00	1.74	7.59	9.16	13.47	17.81	11.09	7.60	6.28	25.27
10.5	10.98	27.59	0.42	0.00	0.78	4.57	6.58	11.05	18.01	14.64	9.71	6.81	27.86
11	13.49	33.15	21.26	0.00	1.34	6.00	7.53	12.11	18.76	13.38	8.70	6.43	25.76
11.5	10.50	27.10	21.22	0.00	0.65	4.55	6.70	11.11	17.58	14.02	9.88	7.97	27.54
12	10.52	29.05	0.42	0.00	0.89	5.23	6.97	10.86	16.89	13.68	9.50	7.27	28.71
12.5	9.11	26.36	0.41	0.00	0.69	4.28	6.81	10.57	15.95	13.90	10.38	7.65	29.76
13	10.00	27.83	0.41	0.00	0.80	4.70	7.01	11.03	16.50	13.63	9.71	7.33	29.30
13.5	8.91	25.64	0.41	0.00	0.61	4.13	6.63	10.36	15.93	14.25	10.97	7.81	29.31
14	7.18	25.87	0.41	0.00	0.72	4.06	7.22	10.83	13.31	12.11	11.11	8.70	31.95
14.5	11.26	29.00	0.42	0.00	0.79	5.00	7.30	11.43	17.28	14.32	10.10	7.30	26.47
15	9.10	24.33	9.53	0.00	0.70	4.02	6.09	9.90	16.07	14.94	10.95	7.14	30.20
15.5	5.93	18.60	0.36	0.00	0.09	2.83	5.13	7.78	11.32	15.41	16.51	8.59	32.35
16	13.57	58.82	21.24	2.32	5.95	3.01	5.93	11.66	17.06	14.43	11.41	10.48	17.74
16.5	13.62	28.09	21.33	0.00	0.58	4.01	7.04	13.80	20.33	14.40	10.53	9.59	19.71
17	11.78	20.06	21.29	0.00	0.00	0.34	6.64	15.34	19.84	15.48	11.26	8.70	22.40
17.5	13.61	29.90	21.30	0.00	0.69	4.69	7.87	13.52	19.11	14.09	9.98	8.49	21.55
18	14.14	29.16	21.33	0.00	0.61	4.22	7.61	14.26	20.05	14.35	10.49	9.14	19.26
18.5	14.47	31.66	21.30	0.00	0.63	5.32	8.83	13.82	18.81	14.11	10.32	8.67	19.50
19	24.96	124.66	24.41	7.69	6.25	7.33	8.79	14.25	16.65	9.63	8.35	8.12	12.95
19.5	21.66	42.58	27.87	0.00	1.48	7.81	11.93	18.00	18.36	9.43	7.82	8.16	17.01
20	21.06	65.07	24.43	5.00	4.99	6.76	10.06	15.63	16.94	8.83	7.15	7.27	17.39
20.5	25.09	89.68	27.87	4.24	5.69	8.15	11.22	15.37	15.39	8.19	7.18	7.86	16.72
21	11.79	35.24	21.30	0.00	1.20	6.49	10.30	12.85	13.47	12.07	11.44	12.34	19.84
21.5	8.44	27.20	21.29	0.00	0.64	4.24	7.96	11.49	13.34	13.40	14.10	11.38	23.46
22	13.97	33.32	24.35	0.00	0.84	5.83	9.36	14.39	16.70	12.05	9.98	10.35	20.51
22.5	18.93	40.54	24.45	0.00	1.58	7.51	10.30	16.45	18.20	10.50	9.16	10.11	16.20
23	19.29	41.71	24.39	0.00	1.66	7.94	10.50	15.98	18.68	11.25	9.72	9.75	14.52
23.5	18.69	40.36	24.37	0.00	1.49	7.43	10.48	15.91	18.71	12.08	10.59	10.37	12.94
24	26.50	96.44	24.48	4.70	5.16	8.51	11.22	16.15	16.74	8.99	7.73	7.93	12.89
24.5	14.80	31.17	24.32	0.00	0.72	4.97	8.29	14.73	19.38	12.36	9.10	8.75	21.70

25	15.81	35.89	21.33	0.00	0.83	6.73	10.05	14.52	18.48	13.29	10.30	9.72	16.09
25.5	15.07	33.10	21.37	0.00	0.79	5.77	9.03	14.24	18.68	12.45	9.14	8.94	20.97
26	10.74	27.38	18.59	0.00	0.79	4.42	6.18	10.75	17.58	16.81	13.63	11.35	18.50
26.5	10.11	26.69	18.59	0.00	0.75	4.31	5.84	10.46	16.96	17.10	15.24	12.87	16.46
27	10.40	26.53	18.61	0.00	0.79	4.23	5.59	10.58	17.86	16.58	13.44	12.04	18.88
27.5	9.50	23.45	18.55	0.00	0.62	3.31	4.63	9.70	17.47	18.66	16.69	12.82	16.10
28	8.44	22.23	16.25	0.00	0.64	3.18	4.19	8.77	16.22	18.42	17.28	12.66	18.64
28.5	7.70	22.95	7.19	0.00	0.60	3.31	5.37	9.56	14.08	16.14	16.63	12.42	21.89
29	9.01	21.20	18.59	0.00	0.50	2.54	4.11	9.75	17.82	18.20	15.82	12.14	19.13
29.5	8.87	22.16	18.60	0.00	0.54	2.84	4.49	10.05	17.01	17.58	16.36	13.05	18.08
30	9.96	21.35	18.57	0.00	0.07	1.61	3.79	9.19	18.28	20.01	17.36	11.65	18.03
30.5	9.60	23.11	18.62	0.00	0.14	3.14	6.28	10.99	17.02	16.44	14.03	11.25	20.72
31	9.55	19.46	18.58	0.00	0.00	1.38	5.60	11.23	17.84	18.49	16.80	12.47	16.19
31.5	11.06	27.19	18.64	0.00	0.72	4.09	6.35	11.85	17.76	16.18	13.70	12.13	17.23
32	10.56	21.91	18.58	0.00	0.19	2.81	4.41	10.36	19.90	19.44	15.63	11.99	15.26
32.5	7.52	18.39	7.19	0.00	0.14	2.23	3.95	8.36	14.41	19.03	20.17	12.49	19.22
33	7.23	20.35	8.23	0.00	0.51	2.64	4.31	8.86	14.84	16.39	16.18	10.52	25.76
33.5	-	-	-	-	-	-	-	-	-	-	-	-	-
34	8.49	30.53	16.25	0.53	2.56	2.03	4.18	9.27	15.55	17.38	16.54	11.96	20.01
34.5	9.51	32.77	21.25	0.49	2.71	2.51	5.15	10.56	17.12	14.68	11.48	9.42	25.90
35	9.68	24.17	21.26	0.00	0.57	3.03	5.53	11.24	16.81	15.68	13.80	12.08	21.28
35.5	8.65	18.58	18.58	0.00	0.14	1.91	3.58	9.42	17.94	19.05	16.94	12.17	18.84
36	10.35	18.67	18.62	0.00	0.11	1.59	3.29	10.19	21.57	19.60	14.36	11.04	18.24
36.5	12.75	18.02	18.67	0.00	0.04	0.66	2.48	11.44	26.85	21.87	16.29	12.31	8.06
37	8.69	19.76	18.66	0.00	0.17	2.25	4.23	10.18	18.37	16.53	13.04	9.62	25.61
37.5	14.16	20.35	21.37	0.00	0.05	0.83	3.71	15.32	26.09	17.64	13.77	12.90	9.70
38	7.99	20.66	9.43	0.00	0.55	2.60	3.87	9.18	15.87	17.91	17.50	12.53	19.99
38.5	7.81	17.20	8.24	0.00	0.10	1.60	3.41	8.86	16.19	19.17	18.93	12.63	19.12
39	10.49	18.54	21.22	0.00	0.09	1.32	3.37	11.36	21.66	18.51	13.66	10.80	19.23
39.5	11.01	19.41	21.22	0.00	0.11	1.53	3.73	11.68	22.02	18.26	13.04	10.50	19.14
40	12.10	21.51	21.30	0.00	0.12	1.86	4.40	14.13	24.47	16.36	10.56	9.08	19.02
40.5	10.57	24.72	21.24	0.00	0.54	3.23	5.82	11.91	18.15	16.35	13.69	11.89	18.43
41	11.24	23.03	21.25	0.00	0.16	2.67	5.60	12.54	19.64	16.87	13.49	11.64	17.40
41.5	10.67	24.69	21.23	0.00	0.56	3.40	5.63	11.33	18.83	16.21	12.31	9.81	21.91
42	12.53	28.09	21.29	0.00	0.59	4.12	7.30	13.15	18.75	14.85	11.46	10.84	18.94
42.5	10.56	26.90	21.28	0.00	0.70	4.18	6.62	11.81	17.63	13.77	9.97	8.62	26.70
43	11.73	27.25	21.28	0.00	0.58	3.85	7.08	12.89	18.05	15.21	12.54	11.78	18.03
43.5	8.77	23.91	21.31	0.00	0.55	3.15	6.11	11.55	16.58	13.64	11.16	9.72	27.55
44	10.11	26.52	21.31	0.00	0.66	3.92	6.80	12.16	16.86	13.66	11.04	10.23	24.67
44.5	10.56	23.97	21.31	0.00	0.17	3.17	6.60	12.65	18.34	13.73	10.00	9.26	26.09
45	10.43	25.88	19.97	0.00	0.52	3.44	6.34	12.21	18.35	14.34	10.68	9.40	24.73
45.5	11.52	25.47	21.26	0.00	0.55	3.49	6.05	12.05	19.46	15.57	11.29	9.47	22.07
46	11.42	24.61	21.24	0.00	0.51	3.22	5.60	11.87	19.84	16.38	12.08	9.82	20.68
46.5	11.94	23.70	21.26	0.00	0.19	3.05	5.53	12.37	20.90	16.11	11.24	9.39	21.21
47	12.37	27.82	21.27	0.00	0.75	4.40	6.16	12.14	19.93	14.94	10.53	9.17	22.00
47.5	13.91	40.73	21.26	0.08	4.32	4.54	5.86	11.66	19.74	14.82	10.25	8.65	20.09
48	12.70	28.33	21.22	0.00	0.74	4.68	6.21	11.66	20.28	15.98	10.75	8.65	21.06
48.5	14.27	27.51	21.27	0.00	0.54	3.68	6.61	13.57	22.14	16.20	11.42	9.80	16.04
49	14.88	30.41	21.25	0.00	0.56	5.00	7.67	13.11	21.42	16.08	11.01	9.17	15.98
49.5	13.84	34.21	21.28	0.00	3.23	3.22	5.44	12.34	21.63	14.80	9.08	7.43	22.83
50	17.01	35.08	21.31	0.00	0.74	4.60	7.27	14.33	22.56	15.56	10.82	9.11	15.02
50.5	20.35	75.89	21.38	3.32	7.00	6.24	7.57	13.56	18.97	12.24	9.73	8.70	12.67
51	14.67	28.83	21.32	0.00	0.72	4.27	6.39	13.72	22.36	14.82	9.85	8.99	18.89
51.5	14.89	24.50	21.27	0.00	0.00	1.78	8.46	14.77	22.70	16.23	10.80	8.92	16.34
52	15.04	38.90	21.25	0.08	4.06	3.84	5.09	12.12	22.77	16.01	10.03	8.20	17.80
52.5	14.58	37.30	21.25	0.08	4.01	3.31	4.53	11.90	23.19	16.03	9.65	7.76	19.53
53	14.21	24.04	21.26	0.00	0.17	2.57	4.92	13.31	24.97	18.67	14.15	12.39	8.85
53.5	12.35	22.74	18.64	0.00	1.24	1.58	3.04	10.47	24.63	20.01	12.35	9.09	17.60
54	13.55	24.87	18.67	0.00	1.34	1.78	3.53	11.70	25.56	20.65	15.35	12.14	7.96
54.5	13.33	17.52	21.22	0.00	0.00	0.07	2.63	12.60	27.72	21.25	15.28	11.81	8.64
55	12.45	16.39	18.64	0.00	0.00	0.00	1.12	10.55	28.94	23.25	16.09	11.69	8.35
55.5	12.91	17.08	21.21	0.00	0.00	0.29	2.29	11.46	27.83	21.19	14.61	11.79	10.53
56	13.93	19.95	21.23	0.00	0.07	1.04	3.09	12.84	27.63	20.90	14.98	11.65	7.78
56.5	13.88	19.71	18.68	0.00	0.07	1.25	2.46	11.95	28.51	22.40	16.18	11.64	5.56
57	12.09	15.36	21.19	0.00	0.00	0.05	1.64	10.40	27.66	20.57	11.74	8.71	19.23
57.5	14.54	19.30	21.24	0.00	0.04	0.81	2.28	12.92	29.93	22.08	15.49	11.10	5.35

58	14.01	18.35	21.30	0.00	0.00	0.33	2.82	13.54	28.40	19.37	13.26	11.54	10.72
58.5	13.00	16.58	21.21	0.00	0.00	0.05	1.88	11.47	28.53	21.74	15.21	11.97	9.16
59	11.76	13.46	18.60	0.00	0.00	0.00	0.06	5.98	30.20	26.23	16.59	11.76	9.19
59.5	14.40	18.16	18.67	0.00	0.04	0.67	1.38	10.77	32.14	24.86	15.93	9.93	4.27
60	10.72	14.64	19.94	0.00	0.00	0.00	1.14	7.22	21.31	18.72	10.91	6.30	34.40
60.5	14.99	18.29	21.38	0.00	0.00	0.06	2.33	15.10	30.01	18.19	12.17	11.11	11.04
61	-	-	-	-	-	-	-	-	-	-	-	-	-
61.5	11.91	16.17	18.64	0.00	0.00	0.06	2.14	10.69	26.17	22.48	16.96	12.61	8.89
62	15.12	19.69	21.31	0.00	0.00	0.57	2.72	14.89	29.48	20.70	15.37	11.32	4.95
62.5	18.36	23.50	24.39	0.00	0.00	0.84	4.40	20.18	30.09	17.24	12.87	10.22	4.16
63	16.54	23.75	24.29	0.00	0.39	1.15	4.01	16.99	28.71	17.50	12.43	10.84	7.99
63.5	18.63	22.62	24.46	0.00	0.00	0.39	3.96	21.23	30.33	15.90	12.02	10.86	5.31
64	-	-	-	-	-	-	-	-	-	-	-	-	-

Table C.2. Wentworth particle size classification showing proportion of particles from each sediment interval of the Smoky 2 core within each category. Categories include clay (4-2 and <2 µm), very fine silt (8-4 µm), fine silt (16-8 µm), medium silt (31-16 µm), coarse silt (63-31 µm), very fine sand (125-63 µm), fine sand (250-125 µm), medium sand (500-250 µm), coarse sand (>500 µm). Also included are the mean, median, and mode for each sediment interval. Cells with dashes represent samples lost during processing. Depths reported are the top measurements of each sediment interval (i.e., depth of 1 cm represents sediment interval 1-1.5 cm).

Depth (cm)	Median (µm)	Mean (µm)	Mode (µm)	>500 µm (%)	500-250 µm (%)	250-125 µm (%)	125-63 µm (%)	63-31 µm (%)	31-16 µm (%)	16-8 µm (%)	8-4 µm (%)	4-2 µm (%)	<2 µm (%)
0	8.47	37.80	6.29	0.00	2.28	11.43	0.73	1.54	10.67	25.89	30.23	13.86	3.36
0.5	6.10	8.89	5.48	0.00	0.00	0.00	0.64	2.80	8.86	23.30	37.48	17.21	9.70
1	6.56	13.35	5.48	0.00	0.00	0.78	3.09	5.40	10.10	21.55	33.55	16.53	9.01
1.5	6.97	13.07	5.48	0.00	0.00	0.43	2.65	6.10	12.13	22.62	32.08	15.89	8.11
2	6.61	15.22	5.48	0.00	0.15	1.77	2.66	4.94	10.28	21.58	33.14	16.86	8.63
2.5	5.42	24.39	4.79	0.11	3.14	1.19	2.34	5.57	8.12	15.64	25.93	17.75	20.20
3	6.04	12.75	5.46	0.00	0.09	1.03	2.25	4.50	8.98	20.16	33.94	18.52	10.53
3.5	5.47	11.16	4.80	0.00	0.06	0.82	1.61	4.38	8.52	18.61	29.99	17.66	18.34
4	5.81	11.60	5.49	0.00	0.07	0.85	1.72	4.58	8.94	20.23	29.45	15.29	18.88
4.5	5.89	12.04	5.49	0.00	0.09	1.01	1.68	4.64	9.25	20.46	29.03	15.06	18.78
5	5.92	12.52	5.49	0.00	0.08	0.96	2.14	5.37	9.38	19.78	28.39	15.27	18.63
5.5	6.82	15.88	5.48	0.00	0.74	0.80	2.12	5.66	11.89	22.00	30.99	15.61	10.21
6	6.01	10.23	5.47	0.00	0.00	0.00	1.42	5.01	10.02	20.63	32.76	17.58	12.58
6.5	4.84	11.70	4.20	0.00	0.06	1.11	2.18	4.73	7.43	14.78	28.37	21.27	20.06
7	-	-	-	-	-	-	-	-	-	-	-	-	-
7.5	5.37	8.84	4.79	0.00	0.00	0.00	1.00	3.81	7.74	18.30	35.17	20.94	13.04
8	4.58	8.49	4.20	0.00	0.05	0.45	0.84	2.91	6.00	14.72	32.15	23.58	19.30
8.5	5.39	9.20	5.50	0.00	0.08	0.64	0.69	2.53	6.54	20.45	32.86	14.81	21.41
9	5.37	8.78	5.48	0.00	0.07	0.58	0.56	1.97	5.78	20.08	36.62	17.65	16.69
9.5	6.14	9.04	6.27	0.00	0.07	0.38	0.32	1.97	7.45	24.95	37.44	13.94	13.47
10	6.90	9.33	6.27	0.00	0.00	0.00	0.23	2.66	11.24	27.79	37.41	13.75	6.93
10.5	6.76	9.00	6.27	0.00	0.00	0.00	0.06	2.26	10.94	27.46	37.63	14.56	7.10
11	5.79	11.33	5.50	0.00	0.13	1.28	1.19	2.71	6.84	21.52	34.67	15.32	16.34
11.5	5.60	11.37	4.80	0.00	0.08	0.96	1.63	3.45	7.96	19.09	34.79	20.38	11.66
12	5.63	6.85	6.27	0.00	0.00	0.00	0.00	0.98	6.02	23.36	37.06	14.20	18.38
12.5	5.46	8.84	5.49	0.00	0.41	0.27	0.06	1.50	6.03	21.68	36.01	16.57	17.47
13	5.33	6.94	6.27	0.00	0.00	0.00	0.00	1.71	6.68	21.73	32.77	14.58	22.54
13.5	6.38	7.87	6.30	0.00	0.00	0.00	0.00	1.30	8.49	27.47	36.15	12.58	14.01
14	5.44	6.76	5.49	0.00	0.00	0.00	0.00	0.82	5.89	21.72	38.58	17.81	15.17
14.5	4.60	8.13	5.50	0.00	0.00	0.00	1.05	4.12	7.43	17.48	24.58	13.48	31.87
15	5.70	7.74	6.74	0.00	0.00	0.00	0.00	0.85	7.00	26.68	32.95	11.98	20.54
15.5	5.26	8.08	5.47	0.00	0.00	0.00	0.45	3.38	8.03	19.62	30.84	17.71	19.98
16	5.42	9.91	5.48	0.00	0.00	0.47	1.45	4.00	7.80	19.39	30.12	16.25	20.52
16.5	5.51	8.24	6.29	0.00	0.00	0.00	0.48	3.54	8.86	21.41	27.68	12.33	25.68
17	5.39	8.63	6.27	0.00	0.00	0.00	0.99	3.82	8.12	20.26	28.81	14.38	23.63
17.5	4.72	8.69	4.79	0.00	0.00	0.00	0.93	4.83	9.08	16.08	25.38	17.51	26.19
18	5.76	11.08	4.80	0.00	0.00	0.00	2.61	5.48	9.27	18.75	30.99	18.94	13.97
18.5	5.65	15.34	4.80	0.00	0.05	1.79	4.47	5.82	7.84	16.87	27.17	16.66	19.33
19	6.42	16.19	7.19	0.00	1.88	0.50	0.44	3.34	10.34	23.79	28.37	11.80	19.54

19.5	6.28	16.22	6.28	0.00	0.50	2.07	2.49	5.71	9.82	19.99	26.20	13.00	20.23
20	5.55	12.22	5.89	0.00	0.08	1.11	1.57	3.94	7.87	18.64	26.80	13.63	26.37
20.5	5.42	12.02	5.48	0.00	0.09	1.18	1.56	4.99	9.46	18.10	25.88	14.76	23.98
21	6.64	10.49	7.21	0.00	0.04	0.17	0.96	4.79	12.10	24.06	26.02	9.86	22.01
21.5	5.37	10.43	6.27	0.00	0.09	0.85	1.09	3.70	8.13	19.80	27.54	13.33	25.47
22	6.03	16.66	6.29	0.00	0.75	2.82	1.66	3.61	8.60	20.97	26.76	11.43	23.41
22.5	5.42	9.23	6.28	0.00	0.40	0.30	0.19	2.20	7.63	21.84	29.69	13.36	24.40
23	6.72	9.91	7.20	0.00	0.00	0.00	0.55	4.74	12.82	24.43	26.89	11.34	19.23
23.5	6.01	8.56	7.18	0.00	0.00	0.00	0.45	3.19	9.67	23.73	29.28	12.17	21.51
24	5.39	9.39	6.27	0.00	0.07	0.54	0.81	3.12	7.55	20.45	29.80	14.36	23.30
24.5	5.21	11.99	5.48	0.00	0.84	0.93	0.83	2.81	6.38	18.73	31.40	16.02	22.07
25	5.68	9.08	6.29	0.00	0.00	0.73	1.87	4.28	8.71	21.18	27.86	11.46	23.91
25.5	3.98	7.55	5.47	0.00	0.00	0.00	1.44	3.34	5.65	14.98	24.38	15.21	35.00
26	8.63	11.38	10.80	0.00	0.00	0.00	0.91	4.30	17.72	30.33	22.05	6.50	18.19
26.5	3.76	5.62	5.48	0.00	0.00	0.00	0.00	1.25	6.38	16.02	24.46	13.77	38.12
27	4.46	13.42	5.48	0.00	0.17	2.33	2.63	3.50	5.50	15.26	24.22	14.09	32.29
27.5	4.34	15.95	4.77	0.00	0.58	2.77	2.39	4.96	7.24	12.76	22.11	17.25	29.95
28	7.00	9.96	8.22	0.00	0.00	0.00	1.04	3.73	11.96	26.98	27.67	7.88	20.75
28.5	4.37	12.39	4.78	0.00	0.10	1.39	2.34	5.55	7.79	13.28	22.67	17.50	29.37
29	3.44	5.58	4.80	0.00	0.00	0.00	0.00	1.81	6.02	14.12	23.38	15.14	39.54
29.5	4.25	9.39	5.47	0.00	0.06	0.88	1.31	3.17	6.04	15.77	24.93	15.67	32.17
30	4.76	9.09	5.98	0.00	0.06	0.37	0.06	1.80	7.85	25.50	31.80	9.01	23.54
30.5	4.36	8.19	5.48	0.00	0.00	0.00	1.00	4.58	7.67	16.25	23.32	14.79	32.39
31	3.73	8.25	4.79	0.00	0.08	0.83	0.72	2.47	5.21	14.18	24.18	17.24	35.11
31.5	5.59	7.59	6.29	0.00	0.00	0.00	0.21	2.22	9.25	22.00	29.29	9.81	27.22
32	5.93	12.94	6.27	0.00	0.11	1.33	2.16	4.97	8.68	20.21	28.04	12.44	22.08
32.5	4.36	5.13	5.50	0.00	0.00	0.00	0.00	0.23	3.11	18.09	32.11	15.24	31.22
33	4.20	5.31	5.50	0.00	0.00	0.00	0.00	0.51	4.14	18.13	29.03	14.63	33.57
33.5	4.05	5.91	6.28	0.00	0.00	0.00	0.00	1.36	6.21	18.28	24.55	13.85	35.74
34	4.20	7.86	6.27	0.00	0.00	0.00	1.05	3.79	7.72	16.79	22.08	13.33	35.25
34.5	-	-	-	-	-	-	-	-	-	-	-	-	-
35	2.84	6.41	3.69	0.00	0.00	0.00	0.21	3.78	6.88	8.86	16.25	19.69	44.34
35.5	2.73	3.03	3.64	0.00	0.00	0.00	0.00	0.00	0.57	2.91	24.17	35.14	37.21
36	3.19	3.86	4.18	0.00	0.00	0.00	0.00	0.34	1.54	7.10	29.69	26.33	35.00
36.5	3.42	3.83	4.19	0.00	0.00	0.00	0.00	0.09	1.02	7.16	32.86	27.29	31.59
37	3.87	5.97	4.79	0.00	0.00	0.00	0.06	2.10	5.57	14.85	26.17	18.29	32.97
37.5	2.24	2.64	2.79	0.00	0.00	0.00	0.00	0.00	0.40	2.19	15.52	37.45	44.44
38	2.40	2.94	3.19	0.00	0.00	0.00	0.00	0.00	0.98	3.17	19.38	34.11	42.36
38.5	2.56	4.25	3.20	0.00	0.05	0.35	0.00	0.40	1.48	5.14	21.31	30.45	40.83
39	1.70	3.14	0.55	0.00	0.00	0.00	0.00	0.27	3.40	4.55	10.51	25.57	55.69
39.5	2.83	3.24	3.65	0.00	0.00	0.00	0.00	0.00	0.80	4.08	25.81	33.03	36.28
40	2.13	2.59	2.78	0.00	0.00	0.00	0.00	0.00	0.98	2.67	14.72	34.97	46.66
40.5	2.32	2.71	3.17	0.00	0.00	0.00	0.00	0.00	0.46	2.42	17.07	36.95	43.10
41	2.42	3.11	3.20	0.00	0.00	0.00	0.00	0.07	1.79	3.70	19.38	31.96	43.09
41.5	2.65	2.96	3.63	0.00	0.00	0.00	0.00	0.00	0.59	2.78	22.68	35.44	38.51
42	2.82	4.38	4.17	0.00	0.00	0.00	0.00	1.37	2.78	8.68	23.57	23.28	40.33
42.5	3.13	4.59	4.19	0.00	0.00	0.00	0.00	1.21	2.92	10.42	25.64	22.00	37.80
43	4.31	4.40	5.47	0.00	0.00	0.00	0.00	0.00	1.45	12.33	40.20	13.50	32.51
43.5	5.86	7.51	6.31	0.00	0.00	0.00	0.70	1.87	5.64	23.98	34.69	7.59	25.54
44	5.53	7.77	6.28	0.00	0.00	0.00	0.83	2.62	6.33	21.14	33.28	9.57	26.23
44.5	5.71	8.03	6.28	0.00	0.04	0.07	0.72	2.44	6.32	22.12	34.80	9.80	23.71
45	5.04	5.35	5.51	0.00	0.00	0.00	0.00	0.00	2.54	17.06	46.96	13.34	20.10
45.5	6.92	16.32	6.27	0.00	1.33	1.62	1.05	2.18	8.00	26.97	41.08	11.91	5.88
46	5.71	6.15	6.28	0.00	0.00	0.00	0.00	0.09	3.88	23.24	42.19	9.36	21.22
46.5	6.13	6.41	7.15	0.00	0.00	0.00	0.00	0.00	3.50	27.36	42.01	7.53	19.59
47	6.53	7.11	7.20	0.00	0.00	0.00	0.00	0.30	5.97	30.28	37.26	6.68	19.52
47.5	5.48	5.88	6.29	0.00	0.00	0.00	0.00	0.11	3.97	22.49	38.62	8.61	26.19
48	6.85	7.61	7.21	0.00	0.00	0.00	0.00	0.41	7.45	31.93	36.29	6.78	17.14
48.5	6.62	7.30	7.21	0.00	0.00	0.00	0.00	0.44	7.11	30.54	34.67	6.48	20.76
49	8.88	11.46	8.24	0.00	0.00	0.00	0.26	3.86	18.45	32.59	29.28	9.80	5.75

Appendix D – X-Ray Fluorescence (XRF)

Table D.1. Average counts of the 20 elements used in the principal component analysis, measured in each sediment interval of the Smoky 4 core. PCA axis 1 (PC1) scores and axis 2 (PC2) scores are included in columns 2 and 3 respectively. Depths reported are the top measurements of each sediment interval (i.e., depth of 1 cm represents sediment interval 1-1.5 cm).

Depth (cm)	PC1	PC2	Al	Si	K	Ca	Ti	V	Cr	Mn	Fe	Ni	Cu	Zn	Br	Rb	Sr	Zr	Sb	Ba	W	Th
0	-1.45	-1.04	56	411	2146	21109	1974	108	144	1136	73512	612	31	430	141	603	3087	581	264	169	715	300
0.5	-2.53	-1.77	45	375	1919	24627	1716	107	131	1410	70372	615	37	394	131	561	3253	493	277	142	690	312
1	-1.54	-2.35	60	389	2009	23029	1850	94	156	1719	73721	619	40	428	132	579	2997	561	278	158	748	308
1.5	-0.22	-2.40	63	528	2552	28983	2181	124	179	1270	80836	514	45	456	108	659	3584	552	296	191	732	234
2	-0.73	-1.74	53	465	2326	26249	2054	109	175	1210	76893	572	54	478	126	727	3530	573	273	193	699	313
2.5	-1.97	-1.52	52	429	2117	25137	1892	108	148	1163	71781	567	41	408	155	610	3500	470	289	167	707	279
3	-2.33	-0.32	58	393	2005	29439	1739	105	145	884	68199	599	67	394	115	576	3561	494	364	167	751	232
3.5	-1.77	-1.21	55	372	2084	29613	1783	104	155	1099	69665	573	60	431	101	569	3620	448	325	178	743	312
4	-0.82	-2.57	53	441	2342	34106	1918	136	180	1185	78297	511	64	457	113	627	4102	516	374	198	752	317
4.5	-1.11	-2.39	62	452	2323	32950	2013	120	200	1291	78820	547	84	491	147	543	3887	494	378	198	734	262
5	-2.51	-1.22	43	350	1979	31115	1741	110	153	1087	70731	527	53	440	147	474	3860	501	375	193	797	153
5.5	-1.42	-0.17	62	388	2151	29407	1886	119	185	794	73013	557	78	433	166	491	3544	605	382	183	812	250
6	-2.94	1.10	43	302	1703	24104	1524	81	145	879	60489	568	77	392	100	490	3321	547	312	157	762	160
6.5	-1.69	-0.28	53	356	1921	26995	1796	105	167	951	66329	571	70	418	119	564	3514	519	329	179	772	325
7	-1.45	-1.15	47	361	2076	30596	1823	129	170	1018	70082	521	67	454	139	669	3776	532	392	191	799	254
7.5	-1.47	-1.20	52	399	2183	30679	1906	120	180	1011	73936	513	78	456	134	670	3639	513	391	197	723	194
8	-0.63	-1.87	60	428	2305	31720	1980	126	175	1122	75677	510	72	489	122	677	3812	537	376	205	766	276
8.5	-1.29	-1.41	50	410	2269	32343	1951	140	168	942	73333	493	74	461	140	601	3979	503	389	186	760	270
9	-1.73	-0.30	54	360	1978	25877	1689	112	167	955	65048	558	69	447	136	484	3437	538	335	187	761	308
9.5	-0.66	-0.40	54	429	2205	27017	2025	112	179	1107	73075	519	100	471	136	565	3465	601	317	192	793	290
10	-0.19	-1.04	58	464	2489	32799	2184	129	200	866	79832	540	77	533	122	747	3634	549	386	205	787	223
10.5	-1.88	0.27	51	357	2011	28960	1822	123	167	803	68248	551	76	434	127	555	3397	499	382	169	811	182
11	-2.35	-0.80	45	328	1990	31729	1722	106	166	1075	69855	545	90	452	158	589	3922	483	416	184	815	209
11.5	-0.99	-2.30	59	466	2435	38022	1999	116	191	1159	81253	492	97	487	137	625	4208	491	421	199	768	236
12	-0.51	-3.02	71	504	2573	37320	2089	140	194	1151	82148	505	82	507	150	667	4165	547	473	225	749	215
12.5	-2.11	-0.88	50	382	2082	33103	1745	112	173	939	70421	515	80	458	156	572	3779	545	376	191	727	187
13	-1.70	0.11	52	358	2029	26029	1751	119	181	979	71656	563	96	433	159	641	3457	446	334	175	802	207
13.5	-0.96	-0.49	65	364	2134	30930	1820	115	180	818	72941	532	83	473	131	742	3666	488	382	176	800	284
14	-2.20	1.16	46	307	1834	27369	1572	114	169	699	70861	559	106	394	125	531	3073	467	378	167	757	249
14.5	-3.71	1.45	36	216	1351	23930	1219	69	138	772	58963	583	51	332	104	422	3038	454	293	138	778	247
15	-2.93	2.09	45	241	1569	20647	1406	92	151	707	61554	578	79	396	150	501	2797	421	283	149	796	189
15.5	-2.20	2.38	36	259	1638	19304	1488	101	164	769	63386	569	94	404	101	606	2677	518	266	147	784	175
16	-3.29	0.91	34	272	1596	23467	1430	94	145	800	61994	549	71	411	174	513	3011	509	290	154	670	255
16.5	-3.59	1.56	41	209	1493	24256	1374	94	135	708	57537	592	64	394	178	537	3164	499	318	121	811	225

17	-3.95	-0.47	42	265	1534	33138	1267	90	138	985	62174	532	76	368	185	424	3604	368	442	165	791	263
17.5	-4.25	0.11	48	258	1424	31806	1228	73	144	924	60771	545	79	368	189	362	3620	472	406	157	777	189
18	-3.68	-0.14	43	286	1591	31169	1364	94	157	1017	61795	538	94	379	179	503	3621	415	407	152	762	214
18.5	-3.45	-1.00	47	249	1581	33272	1402	95	155	1070	65551	514	78	403	164	473	4023	457	430	156	792	207
19	-2.92	-2.23	60	359	1885	40196	1537	105	165	1257	70791	523	113	425	197	610	4449	435	509	189	804	215
19.5	-4.96	-1.64	38	240	1390	38545	1115	83	123	1259	61031	554	78	364	156	483	4199	367	506	153	780	168
20	-4.48	-4.14	49	318	1605	47924	1251	90	136	1362	68442	497	65	395	175	477	5218	389	595	183	778	230
20.5	-3.58	-2.90	54	337	1718	39739	1401	103	166	1345	69546	537	80	390	144	458	4737	450	496	182	773	162
21	-4.02	-0.33	39	247	1403	28822	1196	80	137	968	56378	527	68	345	113	517	4012	446	377	150	712	239
21.5	-2.10	-2.01	61	405	2158	36932	1735	111	164	1039	74936	495	80	481	158	514	4079	437	416	189	720	226
22	-2.82	-0.64	52	336	1819	30324	1520	95	158	892	64453	552	69	411	166	581	3724	378	378	151	744	331
22.5	-2.94	-2.27	58	402	1972	42148	1618	97	170	988	73010	485	83	397	156	545	4391	437	500	189	724	194
23	-3.45	-2.59	53	358	1823	41837	1547	91	160	1092	71052	525	60	415	164	490	4344	439	533	177	773	220
23.5	-3.50	-1.79	53	328	1627	34354	1422	97	147	1075	66007	529	40	368	123	448	3863	482	459	161	744	175
24	-4.01	-0.84	42	255	1450	31284	1268	80	137	1103	62472	538	52	353	135	475	3758	433	398	140	772	194
24.5	-3.41	-3.23	55	406	1920	45067	1514	99	159	1221	71394	519	68	420	172	488	4704	503	535	188	777	184
25	-2.51	-3.13	53	400	1985	38103	1619	97	167	1343	73857	537	67	404	143	671	4216	469	472	192	729	276
25.5	-1.19	-2.73	64	472	2199	38417	1821	114	175	1157	76848	477	68	476	132	678	4083	545	457	191	760	244
26	-1.74	0.03	58	380	1952	25401	1694	102	168	993	67889	529	88	387	105	527	3457	588	334	171	750	203
26.5	-0.94	-1.63	53	430	2202	28727	1883	111	175	1314	72061	551	81	459	98	612	3627	508	353	193	763	337
27	-0.53	0.45	59	432	2269	22955	1991	125	166	860	73292	542	87	486	124	622	3171	547	286	186	774	231
27.5	-0.37	0.47	63	455	2345	23072	2028	122	177	913	73502	575	107	476	123	620	3214	486	300	198	788	277
28	0.06	0.56	60	469	2396	21951	2078	113	199	918	73990	549	104	500	151	710	3060	585	279	185	785	305
28.5	1.88	-1.64	69	597	2854	24670	2469	136	238	1056	87502	500	79	579	132	758	3268	589	315	241	748	324
29	1.87	-1.17	67	583	2825	23579	2481	156	222	1050	86485	556	78	563	110	904	3076	593	289	226	761	273
29.5	0.23	1.15	57	455	2308	20219	2060	114	186	923	75280	542	104	494	110	672	2858	646	241	197	804	212
30	1.36	-0.01	53	534	2630	19822	2350	147	219	1043	80215	573	97	577	124	791	2941	577	226	219	767	311
30.5	-0.37	1.28	54	417	2101	18719	1883	112	160	844	69699	528	92	468	117	715	2824	640	238	175	758	265
31	2.51	-1.04	67	583	2827	22726	2555	154	223	1039	87388	505	80	590	86	795	3018	664	269	236	768	309
31.5	0.43	0.63	60	474	2399	17519	2137	122	203	890	74868	548	69	516	137	669	2705	528	207	190	781	271
32	2.57	0.16	61	560	2758	15503	2510	159	230	1014	86336	556	84	582	113	928	2448	605	200	213	787	306
32.5	1.67	-0.58	64	591	2737	22675	2346	145	217	987	84455	498	89	574	146	744	3034	606	282	236	790	268
33	3.25	-1.56	81	708	3210	23817	2780	149	239	1061	92515	495	89	632	88	911	3215	668	273	262	737	216
33.5	-0.20	1.19	60	479	2407	19707	2156	107	175	831	73588	546	97	518	179	748	2754	618	248	182	772	213
34	0.93	0.48	60	487	2428	20294	2227	141	202	916	77202	538	92	512	103	766	2834	569	253	197	784	270
34.5	0.17	-0.09	65	494	2504	25897	2167	118	184	952	78273	551	101	500	163	676	3074	549	319	216	803	310
35	-0.91	-0.43	52	456	2286	26551	2035	125	181	913	75920	548	81	489	175	611	3328	534	338	198	760	272
35.5	0.78	0.58	55	454	2564	20779	2319	129	186	1035	80772	540	114	525	118	721	2812	585	264	207	800	264
36	2.67	-0.69	66	634	2990	22464	2575	145	244	1017	86462	471	99	566	121	884	2980	681	270	257	765	257
36.5	2.65	0.14	72	646	2984	17349	2692	135	213	1089	81842	538	109	567	105	842	2624	699	223	239	770	297
37	2.37	1.18	58	521	2667	13505	2458	158	234	995	80700	549	102	577	121	775	2197	686	173	220	804	270
37.5	4.36	0.44	64	721	3082	12538	2939	153	262	979	83450	493	78	587	98	865	2419	876	155	253	837	337
38	3.44	1.64	63	668	3044	12284	2847	150	247	793	79868	551	99	616	115	907	2194	722	144	229	806	291

38.5	3.10	0.98	63	634	2869	14501	2659	144	224	980	77152	509	109	576	100	896	2515	824	179	239	790	299
39	2.11	0.81	68	613	2801	16697	2559	151	186	858	78905	541	95	544	90	770	2566	629	195	198	762	326
39.5	1.52	0.67	67	618	2697	16334	2468	109	207	858	75056	516	68	509	105	674	2626	654	181	221	758	277
40	1.70	0.85	60	554	2669	21799	2303	149	223	843	82353	502	128	568	142	795	3043	605	275	222	841	239
40.5	-0.36	1.40	45	425	2316	21406	2082	119	181	991	72289	529	122	487	165	603	2836	580	256	185	841	240
41	-0.37	1.33	45	414	2266	22616	1974	107	195	781	71995	540	99	474	118	676	3005	646	281	181	797	262
41.5	-1.35	0.91	56	410	2109	25017	1825	106	170	860	69173	558	101	429	144	600	3059	560	312	184	779	215
42	-1.84	1.48	57	372	1990	25153	1722	86	154	868	67285	549	116	428	120	493	3131	450	311	174	820	181
42.5	-1.83	1.43	40	366	1931	23388	1718	101	153	887	64916	527	100	421	172	657	2944	543	288	177	806	211
43	-2.98	2.23	45	286	1664	22520	1442	89	140	729	60374	556	86	384	130	416	2872	584	297	134	799	132
43.5	-1.81	0.72	54	389	2007	29582	1684	102	145	843	69193	481	120	402	156	614	3496	570	360	187	789	185
44	-2.62	2.09	53	333	1746	27636	1492	78	142	617	62006	535	104	395	121	415	3187	544	346	172	823	160
44.5	-2.05	1.08	46	361	1899	26796	1626	83	140	746	65110	478	79	426	144	594	3185	513	340	166	819	210
45	-1.79	0.47	46	423	2135	27126	1773	107	159	856	67647	479	79	425	158	540	3133	541	339	173	782	173
45.5	-1.33	-0.61	59	499	2379	33632	1960	107	180	948	74687	491	103	443	195	547	3602	514	388	204	802	210
46	-2.05	1.18	45	379	1948	26897	1684	94	172	794	65523	531	94	418	173	514	3263	495	328	174	849	228
46.5	-0.85	0.70	44	464	2292	28115	1990	107	177	927	73516	516	122	447	137	589	3285	552	315	207	800	240
47	-1.75	1.74	52	349	1842	25036	1593	100	166	732	65580	538	122	548	167	577	3074	514	318	168	778	206
47.5	-2.46	1.89	39	325	1767	27010	1530	84	164	630	61459	522	88	431	122	488	3080	518	324	161	800	189
48	-1.23	0.82	54	411	2189	30072	1809	98	165	682	71230	530	101	464	136	628	3634	650	373	180	836	221
48.5	-1.85	1.52	43	398	1999	24042	1768	94	159	740	66186	542	79	440	139	516	2991	590	311	181	816	155
49	-2.91	2.30	40	327	1715	26198	1477	74	143	611	60394	533	96	374	129	494	3006	544	351	166	813	159
49.5	-2.65	2.42	43	301	1577	22782	1413	70	133	794	59995	530	107	386	112	477	2959	577	268	154	800	175
50	-3.27	2.24	47	326	1663	26951	1359	64	127	600	55553	555	97	365	93	445	3198	498	335	148	773	206
50.5	-2.68	2.70	50	348	1710	23913	1451	86	134	567	57072	525	110	382	143	483	2965	540	319	149	802	189
51	-3.02	2.43	52	333	1716	25744	1433	67	145	593	58512	558	98	394	157	494	3043	556	317	162	806	135
51.5	-2.92	2.05	44	327	1643	24250	1544	70	146	736	55996	517	90	371	141	491	2942	603	299	144	771	168
52	-1.97	2.15	47	347	1738	21389	1522	85	152	843	60496	548	111	422	135	571	2944	585	252	171	798	209
52.5	-1.52	2.31	55	387	1855	19513	1629	77	145	650	58434	490	95	444	123	490	2802	618	238	171	747	243
53	0.96	2.51	52	517	2353	15622	2176	90	201	745	66517	518	101	514	137	719	2399	806	182	186	830	320
53.5	0.98	2.69	55	508	2298	16547	2064	120	163	737	66785	485	121	484	93	858	2408	732	208	187	814	226
54	1.47	1.98	48	569	2475	15852	2257	99	198	784	66209	503	80	559	86	678	2359	853	185	200	800	322
54.5	-0.51	3.08	41	430	2083	15332	1831	84	173	928	60017	520	130	447	121	614	2234	751	208	173	804	235
55	2.50	1.29	56	636	2799	15525	2469	109	201	994	73039	496	105	532	56	865	2462	820	190	231	785	306
55.5	1.91	3.38	58	626	2501	12543	2318	94	174	863	65549	501	171	607	98	739	2188	836	148	213	761	309
56	8.20	-2.58	96	1008	4122	17188	3696	205	286	1020	100832	479	57	674	58	1263	2914	1032	218	342	792	474
56.5	7.66	-0.94	73	965	4169	15780	3823	183	288	964	99640	522	77	741	39	1008	2806	1077	175	319	854	432
57	5.43	-0.23	68	846	3468	16109	3153	170	211	953	88687	508	53	605	58	802	2684	1044	190	275	930	418
57.5	5.49	1.19	72	832	3540	12896	3280	107	241	895	84260	455	104	618	71	948	2541	959	174	294	913	345
58	7.64	1.03	91	864	3691	9889	3555	160	273	816	90936	485	90	702	16	1079	2352	1092	123	310	922	303
58.5	6.96	-0.05	87	923	3916	12616	3507	148	259	890	92998	468	78	658	104	1122	2586	1090	176	316	906	349
59	8.10	-0.30	85	1002	3950	11000	3792	205	282	972	97024	498	96	708	67	860	2294	1142	125	365	825	418
59.5	9.08	-0.52	79	984	4061	9784	3972	180	303	1024	98071	399	94	740	82	1301	2268	1129	125	386	839	393

60	10.56	-1.93	79	967	4273	9276	4103	211	347	1048	99115	492	45	792	8	1374	2539	1252	133	388	845	615
60.5	9.42	-0.23	96	1031	4279	10708	3900	226	293	1080	96507	485	122	753	97	1267	2393	1113	127	400	931	321
61	11.25	-1.94	111	970	4306	9489	4148	213	348	985	102038	480	51	808	0	1197	2550	1126	99	431	881	586
61.5	9.87	-0.61	106	979	4293	9734	3978	197	311	979	98736	481	94	749	34	1061	2395	1147	92	372	875	507
62	9.76	0.38	93	1007	4179	9302	3916	198	283	936	94271	502	96	791	18	1165	2399	1244	128	371	985	406
62.5	7.77	2.16	61	882	3693	8515	3505	177	255	719	88667	453	132	690	68	1048	2483	1216	114	327	968	455
63	8.50	0.63	100	1016	4000	9374	3664	165	286	874	87641	537	78	726	14	999	2472	1245	123	350	962	346

Table D.2. Average counts of the 20 elements used in the principal component analysis, measured in each sediment interval of the Smoky 2 core. PCA axis 1 (PC1) scores and axis 2 (PC2) scores are included in columns 2 and 3 respectively. Depths reported are the top measurements of each sediment interval (i.e., depth of 1 cm represents sediment interval 1-1.5 cm).

Depth (cm)	PC1	PC2	Al	Si	K	Ca	Ti	V	Cr	Mn	Fe	Ni	Cu	Zn	Br	Rb	Sr	Zr	Sb	Ba	W	Th
0	-6.28	0.64	32	277	1924	1296	2145	138	230	380	84342	566	79	450	140	942	914	719	29	164	786	201
0.5	-8.13	-1.71	24	219	1599	1433	1892	135	182	306	72310	732	94	591	139	556	992	691	30	122	851	68
1	-5.51	-1.93	50	310	2075	1729	2276	172	253	334	78468	594	92	565	133	912	1041	625	37	156	942	364
1.5	-5.18	-0.77	46	273	2036	1673	2226	151	211	325	80143	541	86	640	64	818	951	701	40	160	852	435
2	-1.30	-1.02	40	441	2816	2222	2984	232	312	345	108016	560	107	740	88	1254	1381	830	26	233	836	521
2.5	-0.36	-0.49	79	651	3375	2155	3437	269	344	380	116410	516	93	719	124	1195	1293	790	33	286	880	156
3	-2.58	-1.02	54	450	2808	1892	2865	187	296	342	98387	546	70	678	17	914	1168	781	40	225	909	351
3.5	-3.35	-2.71	63	411	2628	1858	2739	195	264	366	87532	569	127	660	107	1041	1129	705	45	210	936	397
4	0.42	1.41	59	617	3470	2381	3589	250	308	435	111660	439	66	771	53	1273	1486	786	26	252	778	321
4.5	0.47	1.82	54	608	3419	2456	3599	267	322	461	108960	448	35	773	85	1239	1424	823	39	269	775	337
5	0.25	0.60	76	633	3409	2497	3429	278	294	468	106165	507	44	758	144	1418	1407	740	35	296	832	386
5.5	-0.62	-1.49	82	545	3176	2222	3324	231	309	472	105138	525	122	734	126	1136	1368	875	15	247	870	332
6	-3.48	-0.33	43	456	2741	2159	2907	217	255	372	100748	567	79	687	85	875	1213	711	29	192	875	80
6.5	-0.94	1.93	73	597	3160	2516	3127	218	305	417	111615	447	15	701	77	1045	1375	612	35	245	854	307
7	-0.52	0.72	52	668	3454	2356	3378	251	320	443	123214	527	54	738	128	1222	1403	661	27	238	863	352
7.5	-1.31	2.54	72	585	3126	2313	3113	242	298	456	118556	463	25	730	70	934	1308	643	18	204	808	119
8	-1.53	2.01	56	558	2919	2469	2989	192	262	433	106947	427	61	687	73	1285	1235	646	31	239	783	253
8.5	-1.88	-0.20	50	508	2873	2380	2932	163	313	470	105655	482	94	738	89	1133	1133	631	55	251	882	242
9	-1.90	0.53	53	513	2848	2354	2966	237	264	497	104339	504	88	723	178	1263	1291	736	35	163	801	325
9.5	-3.52	0.24	37	403	2561	2455	2754	185	252	422	97843	532	74	669	93	827	1206	672	49	201	846	145
10	-2.91	-0.78	60	451	2668	2119	2788	236	244	441	93995	629	75	757	96	997	1221	663	37	197	837	264
10.5	-3.43	0.07	47	418	2621	2044	2629	183	244	408	92281	538	75	660	7	704	1228	633	27	185	826	343
11	-2.65	-0.44	67	509	3001	2519	3014	209	231	529	100998	543	94	751	178	961	1114	486	28	185	873	441
11.5	-3.29	-1.75	68	405	2651	2162	2638	157	270	467	92903	634	78	723	116	950	1117	674	38	226	916	350
12	-2.64	-0.07	50	418	2586	2153	2670	209	233	455	96143	535	79	730	45	919	1295	720	30	195	820	334
12.5	-2.34	-0.38	59	457	2745	2172	2791	185	306	462	103061	535	62	763	73	1033	1211	753	21	189	912	254
13	0.45	2.09	80	613	3158	2563	3213	204	324	517	119935	432	53	783	83	1424	1393	665	29	227	780	399
13.5	-2.81	-0.89	62	367	2475	2353	2600	163	239	416	100650	556	86	731	105	1247	1315	712	41	184	883	360
14	-4.90	0.36	48	355	2307	1664	2511	156	257	381	94020	518	63	646	141	606	1106	600	37	143	864	372

14.5	-0.36	0.89	71	651	3244	2543	3255	221	333	466	118113	417	95	758	107	955	1195	718	26	263	834	267
15	-3.58	0.87	62	461	2529	2321	2506	179	253	378	96176	540	89	670	140	996	1182	639	20	171	765	238
15.5	-2.80	-1.33	62	432	2576	2094	2596	195	275	517	97905	540	145	726	95	932	1164	468	25	205	860	426
16	-3.99	0.46	51	378	2387	2270	2466	145	260	435	93532	518	64	678	92	829	1091	660	39	164	848	235
16.5	-4.40	-0.04	47	363	2260	2184	2401	173	243	412	88575	602	33	748	132	907	1159	747	30	174	880	177
17	-4.57	0.43	47	320	2134	2237	2211	144	213	417	88415	517	58	664	89	836	1122	683	49	182	846	198
17.5	-3.18	0.28	62	371	2351	2425	2504	225	249	383	95695	576	64	698	114	1000	1219	675	42	155	798	381
18	-3.91	-0.66	49	380	2427	1890	2570	192	211	375	96507	631	62	669	45	1155	1209	752	15	147	863	310
18.5	-2.75	0.97	59	414	2656	2280	2722	170	267	398	107191	500	59	675	97	984	1207	641	39	200	829	368
19	-2.92	-0.22	59	468	2685	2173	2788	191	288	379	106485	537	78	723	99	1061	1254	616	28	196	902	186
19.5	2.11	0.95	98	698	3529	2839	3612	267	334	519	124980	481	54	867	112	1461	1601	718	49	303	816	327
20	-1.27	1.36	66	496	2985	2342	3032	210	311	431	113761	477	65	771	108	1129	1273	542	32	244	815	373
20.5	-2.12	-0.65	51	452	2759	2076	2757	224	268	500	110812	590	100	735	108	1136	1124	753	40	216	827	324
21	-1.72	-0.24	59	522	3156	2569	3149	223	271	473	111658	571	99	777	104	1038	1245	535	21	204	839	375
21.5	-1.22	1.22	76	496	2998	2374	3038	203	322	487	111288	511	26	770	131	1124	1270	677	36	206	848	375
22	-2.30	-0.22	74	481	2861	2010	2966	199	272	447	101983	573	123	760	72	801	1169	673	33	240	756	134
22.5	-0.41	-0.66	82	592	3200	2471	3246	216	285	452	107732	491	129	748	72	1303	1400	683	25	264	837	246
23	-1.90	0.68	77	459	2857	2323	3066	255	251	421	98573	535	41	728	75	1101	1307	806	28	191	823	126
23.5	-1.62	0.89	56	469	3001	2021	3212	187	296	459	100265	502	71	718	76	1194	1355	607	31	211	790	424
24	-3.69	0.83	42	433	2624	1862	2767	170	261	366	92893	489	78	640	110	886	1240	695	21	209	807	238
24.5	0.16	1.14	73	603	3359	2376	3411	249	293	453	115608	473	57	737	116	1241	1498	785	55	240	786	351
25	-3.08	-2.50	80	455	2702	2245	2763	175	283	470	97165	628	152	703	106	773	1147	647	27	187	877	266
25.5	-3.35	-0.89	73	408	2534	2066	2631	189	206	447	95174	532	120	677	51	872	1132	545	34	201	850	302
26	-4.77	0.68	46	362	2314	2058	2447	180	241	372	91023	621	27	655	99	843	1150	647	13	150	837	267
26.5	-1.61	1.59	57	521	2956	2510	2954	223	284	373	107186	484	42	723	100	1173	1316	661	40	219	805	311
27	-3.67	-0.40	44	445	2692	2097	2730	175	229	413	100510	559	121	625	89	915	1214	472	41	177	815	394
27.5	-2.34	-1.33	55	508	2944	2152	2926	205	273	452	105552	544	111	771	146	1153	1358	713	15	195	919	258
28	-1.14	0.89	69	577	3115	2281	3121	222	281	464	116622	562	62	778	81	1195	1340	704	16	218	801	215
28.5	-0.28	-0.80	77	581	3283	2407	3291	247	290	522	118881	600	103	817	92	1232	1507	627	25	222	842	329
29	-1.02	1.16	65	560	3020	2329	3003	216	277	556	114293	521	74	821	142	1377	1343	625	32	225	787	206
29.5	0.47	0.91	72	583	3206	2585	3111	254	308	502	126471	567	75	864	100	1403	1386	719	42	247	751	335
30	0.61	1.45	96	711	3361	2115	3381	227	311	560	122409	406	63	770	128	1233	1436	708	35	224	824	383
30.5	1.16	1.39	93	704	3391	2728	3413	249	306	566	136222	414	93	861	106	1031	1400	632	26	242	807	364
31	1.92	1.96	80	710	3439	2641	3545	236	348	563	145355	458	75	843	46	1282	1430	693	32	253	766	355
31.5	2.67	2.49	79	812	3745	2674	3668	254	352	585	140022	316	78	948	112	1216	1491	730	31	296	789	296
32	2.28	1.88	80	801	3776	2543	3715	256	340	517	130351	386	75	858	28	1281	1472	738	32	278	777	302
32.5	3.42	1.06	101	860	4119	2816	3982	270	315	605	125578	419	81	961	49	1396	1552	759	40	278	774	356
33	5.48	-0.67	104	984	4332	3292	4227	341	351	646	124610	442	75	1077	38	1534	1880	803	49	320	879	417
33.5	5.41	-1.74	114	1000	4399	2971	4272	322	370	627	117582	511	95	1010	51	1548	1903	878	48	353	861	468
34	4.30	-1.55	106	965	4288	3281	4338	267	367	510	108278	473	74	945	62	1571	1848	1048	41	347	911	224
34.5	4.22	-1.53	114	857	4110	3378	4126	280	320	586	119362	526	104	936	19	1577	1818	896	47	286	845	342
35	3.68	-2.14	98	948	4304	2732	4229	306	381	543	120207	528	104	1060	68	1224	1590	800	16	357	935	386
35.5	2.68	-0.61	83	836	4133	2689	3897	273	321	567	119659	463	75	997	49	1306	1668	740	36	307	910	294

36	4.66	0.58	106	908	4282	3040	4121	313	359	603	133985	470	105	1016	65	1581	1758	684	15	330	768	385
36.5	3.43	-0.35	80	906	4244	2574	4130	305	344	536	126751	469	89	1040	58	1491	1658	702	16	302	872	438
37	4.52	1.95	102	949	4306	2933	4102	287	357	521	127049	402	49	927	43	1728	1721	748	39	313	754	437
37.5	5.19	-0.73	102	972	4576	2573	4454	342	389	601	120924	530	73	1025	10	1676	1797	766	27	367	841	386
38	5.88	0.79	89	935	4560	3462	4395	334	385	544	127089	407	75	961	1	1732	1797	824	38	371	785	444
38.5	4.68	0.46	112	943	4520	3350	4354	283	391	564	122449	465	73	930	86	1331	1670	802	33	339	785	488
39	3.81	-2.16	109	916	4505	2597	4304	347	327	567	120575	564	137	919	82	1421	1749	758	44	349	843	299
39.5	2.78	-0.95	105	889	4282	3377	4107	312	344	497	116617	514	92	750	80	1301	1475	711	37	322	878	358
40	3.83	-0.76	97	903	4349	2985	4221	310	341	462	112337	493	69	915	15	1686	1839	687	43	318	877	429
40.5	3.83	0.51	91	909	4372	3595	4245	291	331	431	117611	367	102	828	55	1390	1686	709	54	338	802	442
41	4.88	0.35	97	919	4481	3510	4351	280	413	460	117607	490	50	933	62	1876	1871	943	26	359	819	274
41.5	3.56	-1.10	92	870	4320	3461	4149	338	352	361	108354	442	128	883	41	1468	1757	740	33	315	841	395
42	2.92	-0.72	111	850	4073	3947	4008	272	344	413	104696	521	72	891	123	1435	1724	730	42	318	853	403
42.5	7.25	-0.70	102	1032	4915	3786	4775	306	379	822	119812	518	95	1177	1	1662	1996	869	27	362	771	387
43	5.06	1.52	89	941	4488	3709	4533	310	396	482	122756	456	57	892	20	1838	1768	593	29	373	768	437
43.5	5.03	-1.10	91	896	4416	3497	4412	292	364	601	120682	476	126	1001	59	1486	1791	880	23	372	812	427
44	4.81	-1.50	93	904	4395	2290	4321	366	368	608	113377	529	114	964	50	1731	1854	800	31	350	808	533
44.5	4.37	-1.76	88	937	4377	2640	4356	284	367	626	115367	546	103	1023	25	1574	1810	730	48	355	862	425
45	4.59	-1.61	112	966	4241	3280	4177	299	328	586	110840	552	110	998	32	1508	1857	876	44	335	798	353
45.5	3.72	-1.06	92	902	4152	3318	4102	273	365	491	105485	496	92	963	68	1469	1872	748	55	325	838	444
46	4.18	-0.25	70	899	4403	2719	4229	283	359	589	113423	496	104	995	13	1642	1754	815	32	337	760	401
46.5	4.40	-0.44	95	899	4256	3173	4176	306	343	602	122114	508	113	1023	37	1285	1758	806	50	310	751	393
47	3.77	1.78	79	807	3971	3205	3905	319	381	552	129974	494	79	901	39	1369	1697	707	33	337	691	313